(4)

TECHNICAL REPORT BRL-TR-2982

BRL

INCREMENTAL DRAG DUE TO GROOVES AND THREADS FOR KE PROJECTILES

AMEER G. MIKHAIL

MARCH 1989

U.S. ARMY LABORATORY COMMAND

BALLISTIC RESEARCH LABORATORY

ABERDEEN PROVING GROUND, MARYLAND

DESTRUCTION NOTICE

Destroy this report when it is no longer needed. DO NOT return it to the originator.

Additional copies of this report may be obtained from the National Technical Information Service, U.S. Department of Commerce, Springfield, VA 22161.

The findings of this report are not to be construed as an official Department of the Army position, unless so designated by other authorized documents.

The use of trade names or manufacturers' names in this report does not constitute indorsement of any commercial product.

UNCLASSIFIED

SECURITY CLASSIFICATION OF THIS PAGE

REPORT DOCUMENTATION PAGE

Form Approved OMB No. 0704-0188

1a. REPORT SECURITY CLASSIFICATION: UNCLASSIFIED	1b. RESTRICTIVE MARKINGS
2a. SECURITY CLASSIFICATION AUTHORITY	3. DISTRIBUTION/AVAILABILITY OF REPORT: Approved for public release, distribution unlimited.
2b. DECLASSIFICATION/DOWNGRADING SCHEDULE	
4. PERFORMING ORGANIZATION REPORT NUMBER(S): BRL-TR-2982	5. MONITORING ORGANIZATION REPORT NUMBER(S)
6a. NAME OF PERFORMING ORGANIZATION: U.S. Army Ballistic Research Laboratory; 6b. OFFICE SYMBOL (If applicable): SLCBR-LF	7a. NAME OF MONITORING ORGANIZATION
6c. ADDRESS (City, State, and ZIP Code): Aberdeen Proving Ground, Maryland 21005-5066	7b. ADDRESS (City, State, and ZIP Code)
8a. NAME OF FUNDING/SPONSORING ORGANIZATION; 8b. OFFICE SYMBOL (If applicable)	9. PROCUREMENT INSTRUMENT IDENTIFICATION NUMBER
8c. ADDRESS (City, State, and ZIP Code)	10. SOURCE OF FUNDING NUMBERS: PROGRAM ELEMENT NO. 62618A; PROJECT NO. 1L162618AH80; TASK NO. 00; WORK UNIT ACCESSION NO. 001 AJ

11. TITLE (Include Security Classification)

INCREMENTAL DRAG DUE TO GROOVES AND THREADS FOR KE PROJECTILES

12. PERSONAL AUTHOR(S)

MIKHAIL, AMEER G.

13a. TYPE OF REPORT	13b. TIME COVERED	14. DATE OF REPORT (Year, Month, Day)	15. PAGE COUNT
Technical Report	FROM _____ TO _____		

16. SUPPLEMENTARY NOTATION

17. COSATI CODES		
FIELD	GROUP	SUB-GROUP
01	01	
19	01	

18. SUBJECT TERMS (Continue on reverse if necessary and identify by block number)

Kinetic Energy Projectiles; Supersonic Flight; Groove Drag; Threads Drag; Buttress Drag; Wind Tunnel Data; Data Correlation; (etc.)

19. ABSTRACT (Continue on reverse if necessary and identify by block number)

A prediction method for estimating the increment of increase in the drag coefficient due to the grooves on the surface of the body of a Kinetic Energy (KE) projectile is established based on wind tunnel data. Known existing methods give very poor results when compared to the experimental data. Twenty cases were considered for the present correlations and validation. The results achieved are very satisfactory. The present analysis considers parameters not included in the existing methods: the groove pitch (or alternately the groove depth); and multi-groove types residing on the same projectile body. The groove drag decreases very rapidly with the increase in Reynolds number and also decreases considerably with the increase in Mach number. The range of validity of the present expressions coincides with the usual KE projectile requirement, which establishes the Mach number range to be $3.5 < M < 5.5$ and $\alpha = 0^0$.

20. DISTRIBUTION/AVAILABILITY OF ABSTRACT	21. ABSTRACT SECURITY CLASSIFICATION
☒ UNCLASSIFIED/UNLIMITED ☐ SAME AS RPT ☐ DTIC USERS	UNCLASSIFIED

22a. NAME OF RESPONSIBLE INDIVIDUAL	22b. TELEPHONE (Include Area Code)	22c. OFFICE SYMBOL
Ameer G. Mikhail	(301) 278-3773	SLCBR-LF-C

DD Form 1473, JUN 86 — Previous editions are obsolete. — SECURITY CLASSIFICATION OF THIS PAGE UNCLASSIFIED

TABLE OF CONTENTS

LIST OF FIGURES

LIST OF FIGURES (Continued)

LIST OF TABLES

I. INTRODUCTION

There are certain types of flight vehicles, namely the Kinetic Energy (KE) projectiles, which must have relatively large body grooves to hold a sabot which functions as a bore-rider inside the gun tube and which separates at a short distance from the muzzle of the gun. These grooves, which usually extend over half of the total length of the projectile, increase the axial force coefficient and therefore the drag. The grooves also affect the aerodynamics of the fins of these projectiles; however, this effect will not be considered in this study.

In recent years, long KE projectiles (those with L/D > 20) have been receiving closer attention due to their terminal ballistics effectiveness. For these long penetrators, the groove drag is an increasingly important component of the total drag of the vehicle. It is for this class of projectiles that a method was needed for predicting the increase in the drag coefficient due to these grooves. Reference 1 offers wind tunnel results for this class of projectiles and represents a basis for validation of the models as well as a basis for a correlation study.

Because the groove drag is small for shorter projectiles (L/D < 20) at Mach number of 5, not many investigations have been carried out for its study. Also, because the effect of grooves on aerodynamics is only of interest to projectile designers, no investigations have been made in the corresponding missile aerodynamics studies. Therefore, most short KE projectiles are currently designed without any consideration to groove drag. Among the available literature on the subject, Reference 2 offers an expression for calculating ΔC_{D_g}, without any basis and without any reference to any experimental data for validation. Reference 3 offers a more logically acceptable expression which is validated using four data points; but which is shown to provide much higher values (300% higher) in comparison with the present wind tunnel data. In addition, Reference 3 does not disclose the Reynolds number of the wind tunnel tests

With only poor prediction capabilities being available, the present work was pursued to fill a void and to provide a prediction capability based on the correlation of the experimental data of Reference 1 as well as other data provided by Reference 4. The results of this correlation will be compared to the predictions of both References 2 and 3.

The present correlations include the direct effect of the groove pitch (or the groove depth, since they are directly related for all standard threads). The present analysis also allows for multiple groove types on the same body. An example for this particular projectile configuration is shown in Figure 1 together with the general nomenclature.

The present work limits itself to zero angle of attack. Therefore, distinction between drag and axial force vanishes and the drag coefficient will be used throughout this report.

II. WIND TUNNEL DATA AND TEST

Reference 1 documents tests performed at the supersonic wind tunnel of the Naval Surface Weapons Center Laboratory at White Oak, Maryland. The tests were performed at Mach numbers 3.5, 4.0 and 5.0, with the majority of tests run at $M = 5.0$. The Reynolds number for the tests varied between 4.0 through 5.8×10^6 per foot ($12.2\text{-}19.0 \times 10^6$ per meter).

All the models had a diameter of 0.94 inch (23.9 mm). The models were sting-supported. Four lengths were tested, with L/D of 20.59, 25.59, 30.58 and 35.59. Both body-alone (without fins) smooth-surface and body-alone grooved-surface configurations were tested.

The groovings are made on two body sections, a forward and a rear section. The forward section is always grooved while the rear was either smooth, threaded or grooved. The notation (G/T) is used to denote Grooved forward section and Threaded rear section. Figure 2 displays the three basic combinations together with the totally smooth body. Tests were also performed with and without fins; however, the present work excludes the cases with fins in order to obtain a better evaluation of the effects of grooves on the axial force coefficient. The grooves were 8 per inch (i.e., pitch = 1/8 inch, or 3.17 mm) while the threads were 32 per inch (pitch = 1/32 inch, or 0.79 mm).

Four different noses were tested and they closely approximate the 10° cone (semi-vertex angle). They are two Sears-Haack noses and a bi-conical shape in addition to the 10° cone. In the present study, the nose configuration does not affect the results since only the drag increase between smooth and grooved configuration, ΔC_{D_g} , is considered. Most of the tests, however, were run with the Sears-Haack nose. This nose configuration and details of the forward and rear grooves are shown in Figure 2b.

Examination of the wind tunnel results of Reference 1 indicated that the measurements are not always perfect and the accuracy of the result may be affected. For example, the axial force coefficient for some cases did not exhibit symmetry for positive and negative α. Some obvious errors for other cases for the normal force existed, usually for negative α. With such long projectiles being supported by a sting from its base, possible rod bending may partially explain the source of asymmetry with respect to α.

Seventeen test cases were identified from the data of Reference 1 and they are listed in Table 1. The total pressure of the wind tunnel varied between 2.4 and 8.2 times the atmospheric value.

A second set of data was obtained from Reference 4. This data consisted of three tests at Mach numbers 3.49, 3.98 and 4.75 with a corresponding tunnel Reynolds number of 12, 14 and 18×10^6 per foot (39.4, 45.9 and 59.1×10^6 per meter), respectively. The tests were run at the Vought Corporation wind tunnel in Dallas, Texas. The wind tunnel model is shown in Figure 3, with grooving of four grooves per inch (pitch = 0.25 inch or 6.35 mm). Both smooth and grooved models were tested. The results and test conditions for these cases are listed in Table 2.

III. ANALYSIS AND CORRELATIONS

1. REVIEW OF EXISTING EXPRESSIONS

A quick review of existing expressions will be presented so that differences and similarities with the present work will be more clear.

Reference 2 provides an empirical relation in the form of:

$$\Delta C_{D_g} = [0.00025\ M^{3.9}\ l_g] \cdot C_{D_{TSB}} \tag{1}$$

where ΔC_{D_g} is the incremental drag coefficient due to grooves, based on the projectile reference area A_{ref} ($= \pi D^2/4$), where D is the reference diameter for the projectile

M is the free stream Mach number of the projectile

l_g is the length of the grooved portion, in calibers

$C_{D_{TSB}}$ is the body-alone total drag coefficient (including base drag) for the smooth body (i.e., without grooves) configuration.

Reference 3 provides the following expression for computing the incremental drag.

$$\Delta C_{D_g} = 1.6 \frac{l_g}{l_c} \cdot C_{D_{SFSB}} \tag{2a}$$

where l_c is the length of the cylindrical portion of the body, in calibers,

$C_{D_{SFSB}}$ is the drag coefficient due to skin friction of the smooth body of the cylindrical portion, l_c, of the body,

$$C_{D_{SFSB}} = (4 d_c l_c) \cdot c_f \ . \tag{2b}$$

The skin friction coefficient, c_f, is defined as:

$$c_f = \frac{\tau}{0.5 \rho_\infty V^2 A_{ref}} \ ,$$

where τ is the skin friction shear stress at the projectile surface

and d_c is the diameter of the cylindrical portion, in calibers.

Reference 3 did not specify the expression used for c_f, in its application to the projectile configuration shown in Figure 4. In this study, an expression for c_f for turbulent flow was used from Reference 5 as:

$$c_f = \frac{0.455(1 + 0.2M_\infty^2)^{-0.32}}{(\log_{10} R_{e_L})^{2.58}} \qquad (2c)$$

where R_{e_L} is the Reynolds number based on the total length of the projectile.

2. PRESENT ANALYSIS

The present approach is similar in general to the data correlation approach used earlier in Reference 6. The influencing physical parameters are first identified then some of the wind tunnel data are used to determine the constants in the correlation. Finally, the rest of the data is used for validation of the obtained expressions.

a. First expression This expression is targeted only for "typical" KE projectiles as shown in Figure 1. More specifically, the "typical" KE projectile is defined as one with nose cone semi-vertex angle less than 9°, having a very small nose radius < 0.03 D, with no boattail, and having one main cylindrical diameter. This expression is not valid for KE projectiles shown in Figure 3. This expression is formulated in the form of Eq. (1) (of Reference 2), where the body-alone, smooth, total body drag coefficient is known, and only the incremental groove drag is required. This approach suits projectile designers where the groove drag is considered after all other design and shape requirements have been fulfilled.

First, considering the physical parameters that do affect the groove drag, one might write:

$$\Delta C_{D_g} = F(M, R_e, l_g, p, h, x_o)$$

where R_e is the Reynolds number per unit length,

p is the groove pitch ($p = 1/n$ where n is the number of grooves per unit length),

h is the depth of the groove,

x_o is the distance from the nose tip to the first groove.

The parameter x_o was neglected based on the results of Reference 3 which indicated no measureable effect on ΔC_{D_g} of slightly varying x_o. Also, the

parameter h was eliminated since both p and h are directly related for all standard groove geometries. Therefore, the expression will be a function of the pitch, p, which also can usually be more easily measured than h. The above expression is then simplified and written as:

$$\Delta C_{D_g} = [F(M, R_e, l_g, p)] \cdot C_{D_{TSB}} \quad .$$

Based on the data for the 17 cases of Reference 1, the first correlation in the present work for typical projectiles is introduced as:

$$\Delta C_{D_g} = \left[2.05\ TF_1 \cdot \frac{l_g}{L} \cdot MF_1 \cdot RF_1\right] \cdot C_{D_{TSB}} \tag{3a}$$

where TF_1 is the Thread Factor defined as:

$$TF_1 = 0.84 + 0.117\left(\frac{p}{0.031}\right) - 0.007\left(\frac{p}{0.031}\right)^2 \tag{3b}$$

where p is the groove pitch in inches,

MF_1 is the Mach number Factor introduced as:

$$MF_1 = \frac{1}{M_\infty(1.453 - 0.067M_\infty)} \quad , \tag{3c}$$

RF_1 is the Reynolds number Factor introduced as:

$$RF_1 = \left(\frac{4.2 \times 10^6}{R_e}\right)^{0.8} \quad , \tag{3d}$$

and R_e is the Reynolds number per foot.

For multiple grooves with different pitch on the same projectile, Eq. (3a) takes the form:

$$\Delta C_{D_g} = \left[2.05\left(\frac{TF_{11}\ l_{g_1} + TF_{12}\ l_{g_2}}{L}\right) \cdot MF_1 \cdot RF_1\right] \cdot C_{D_{TSB}} \tag{4}$$

where TF_{11} and TF_{12} are the thread factors for the threads of pitch p_1 and p_2, respectively.

One can notice the large differences between the expression of Eq. (3a) and the expression of Eq. (1) of Reference 2. The latter does not include Reynolds number dependence or groove pitch dependence. Further, ΔC_{D_g} increases with the increase in Mach number, while in reality it decreases with Mach number. Also, Eq. (1) depends directly on l_g while Eq. (3a) is found to be more appropriate if l_g/L is used.

Finally, Eq. (1) is found, as will be shown in the results, to give results as high as 10 times the experimental value. Equation (3a) follows the data within ±13%.

b. Second expression For non-typical KE projectiles, as shown in Figure 3, it is not adequate to use $\Delta C_{D_{TSB}}$ as an input. This is because large variations in nose or boattail angles can cause large changes in $\Delta C_{D_{TSB}}$ even though the groove drag on the bodies will not change.

Therefore, an approach like that of Reference 3, which relates only to the cylindrical part of the projectile (i.e., excluding the nose and the boattail), should be more appropriate. Therefore, this expression is targeted to be more general than that of Eq. (3).

Based on the data of References 1 and 4, the second correlation for the general projectile configuration was found to have the form:

$$\Delta C_{D_g} = \left[2.59\ TF_2 \cdot \frac{l_g}{l_c} \cdot MF_2 \cdot RF_2 \right] \cdot C_{D_{SFSB}} \tag{5a}$$

where

$$TF_2 = \left(1 + 0.1 \left(\frac{p}{0.031} \right)^a \right) , \tag{5b}$$

$$a = 0.528 \left(\frac{p}{0.031} \right)^{0.462} ,$$

$$MF_2 = M^{-[3.164 + 3.225\ M^{0.4} - 0.156\ M^{1.5}]} , \tag{5c}$$

$$RF_2 = \left(\frac{9 \times 10^6}{R_{e_L}} \right)^{0.6} , \tag{5d}$$

and $C_{D_{SFSB}}$ is as given by Eq. (2b).

For configurations with multiple thread types, Equation (5a) becomes:

$$\Delta C_{D_g} = 2.59 \cdot \left(\frac{TF_{21}\, l_{g_1} + TF_{22}\, l_{g_2}}{l_c} \right) \cdot MF_2 \cdot RF_2 \cdot C_{D_{SFSB}} \cdot \qquad (6)$$

Comparison of the present expression of Eq. (5) and that of Eq. (2) (i.e., expression of Reference 3) reveals the following facts. First, the present analysis includes explicitly the effects of Mach number, groove pitch and Reynolds number. None of these effects is considered by Reference 3. Second, as will be shown, the results of applying the expression of Reference 3, in general, overpredict the wind tunnel data by 300%.

Since the second correlation expression (Eq. (5)) is more general, i.e., can be applied to all KE configurations (including the configuration of Figure 3), it is recommended over the first correlation expression. However, in cases where both expressions apply, the results of those two expressions should be very close to each other.

IV. RESULTS AND COMPARISONS

Equation (3) of the first expression was first applied to the configurations of Reference 1. Seventeen cases were computed. Also the expressions of References 2 and 3 were applied and compared with the experimental data.

Figures 5a-d show the variation of the incremental drag with the increase of Mach number for the four different L/D's of 20, 25, 30 and 35, respectively. Figure 5a shows the predictions of Reference 3 to be twice as high as the data, while those of Reference 2 are much higher. Also, the trend given by the expression of Eq. (1) of Reference 2 is in the wrong direction compared to the data. Figures 5b-d all show the same features as stated above and also indicate the accuracy of the present correlation.

Figures 6a-c show the effect of the length of the projectile (and hence the length of the grooved section) on the incremental drag, for each of the Mach numbers of 3.5, 4.0 and 5.0. The expressions of References 2 and 3 overpredict the results by more than 100% as seen in Figure 6a. The same results are repeated in Figures 6b and 6c. In all cases, the present correlation predicts the results very accurately. It is of interest to notice that in Figure 6c, Eq. (1) of Reference 2 overpredicts ΔC_{D_g} by more than ten times for L/D = 35.

Figures 7a-d focus on the variation of l_g/L, at Mach 5.0 where most of the tests of Reference 1 were made for the same four L/D's of 20, 25, 30 and 35. The same good agreement between present expression predictions and the experimental data persist. Also, one notices the considerable and consistent overprediction of the expressions of References 2 and 3 being evident.

Figures 8a-d re-cap the results as variation of the incremental drag with the groove type. The same agreement with the data persists for the present expressions while the expressions of Reference 2 and 3 consistently overpredict the results as shown in Figure 8a. Figures 8b-d gives the same trend described above.

A summary of the present predictions of Eq. (3), and the wind tunnel data of References 1 and 4 is given in Table 3.

The second expression, Eq. (5), was applied to the test case of Reference 4 where the first expression, Eq. (3), is not applicable. The results as shown in Figure 9 are in good agreement considering the complexity of the shape. It is to be noted that the present results underpredict the data. This underprediction is expected since the grooves are known to increase the boattail drag.[7] This trend has also been shown in Reference 7 where serrated body ends were tested in wind tunnels at subsonic speeds, causing an increase in the base drag. The effect of grooves on boattail drag is not included in this study; however, this effect explains why the present predictions for this projectile configuration must be smaller than those of the wind tunnel.

The second expression, Eq. (5), was then applied to some of the cases of Reference 1 to see how closely the two correlation expressions compare. Nine of the seventeen cases were recomputed and the results were very similar. Those results and a comparison with the earlier results of the first expression, Eq. (3), are tabulated in Table 4.

A summary plot for the comparison of the present two prediction correlations, Eqs. (3) and (5), with the wind tunnel data is given by Figure 10. The predictions are shown to be in good agreement with the data.

It is felt that the most influential factor is the Reynolds number, followed by the Mach number. The incremental groove drag decrease significantly with increase in Reynolds number. It also increases rapidly with the decrease of Mach number towards the sonic value. The present correlations are only to be used for $M > 3.5$ since Mach number function was targeted for that region only. It is found that for $M < 3.5$ the Mach number function may greatly overpredict the expected answer.

V. SUMMARY AND CONCLUSIONS

A fast prediction capability for computing the incremental drag of Kinetic Energy projectiles due to surface grooves at supersonic speeds has been established.

Physical variables affecting the groove drag have been identified and studied with respect to their importance.

Two correlations with wind tunnel data are established for typical and general KE projectile configurations. The second correlation is recommended since it can be applied to many KE projectile configurations. The correlation expressions are valid only for the Mach range $3.5 < M < 5.5$ and for $\alpha = 0°$. Any application for Mach numbers less than 3.5 will yield overpredicted results.

Comparison with other existing prediction expressions heavily favored the present correlations. The accuracy of these present correlations is ±20% while the existing prediction methods of References 2 and 3 can be as high as +1000% and +300%, respectively.

Finally, the Reynolds number is expected to play a significant role. The incremental drag decreases significantly with the increase of Reynolds number. It is hoped that more tests will be available at the Reynolds number of 35×10^6 per foot rather than the present values of $4\text{-}6 \times 10^6$ per foot. These tests could be run in cryogenic wind tunnels and the results further used to validate the present correlations.

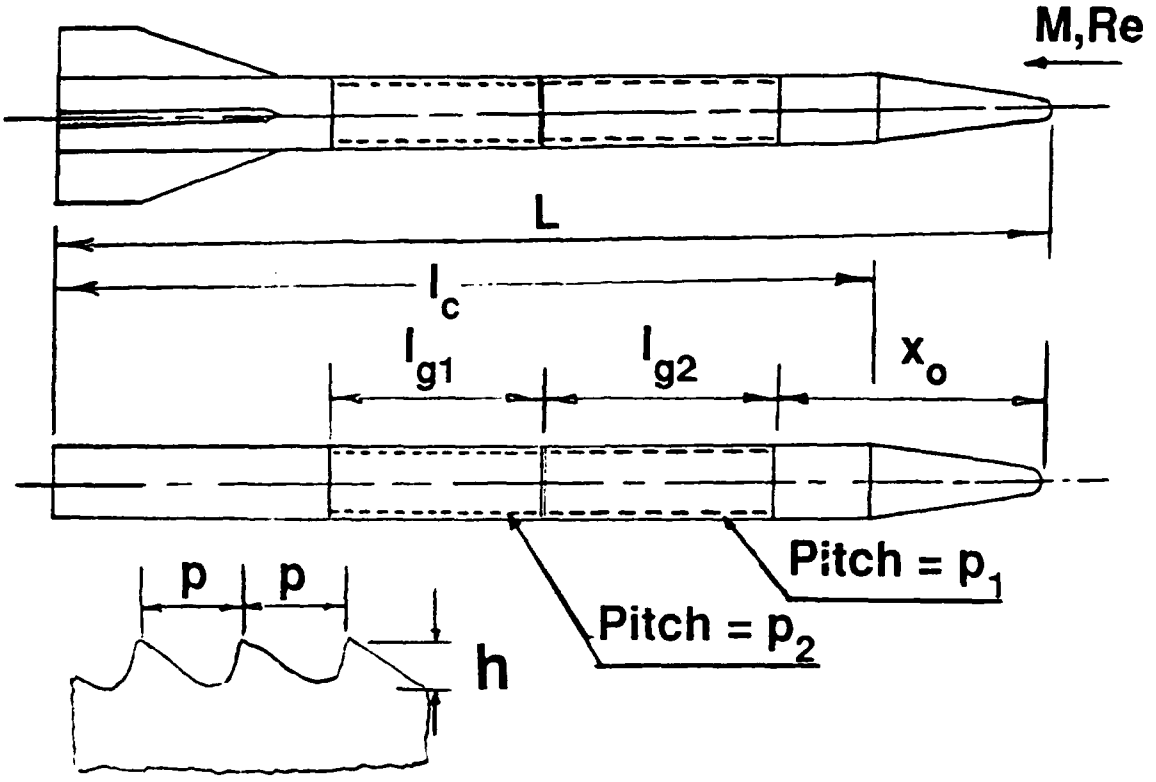

Figure 1. General configuration and nomenclature for a Kinetic Energy projectile.

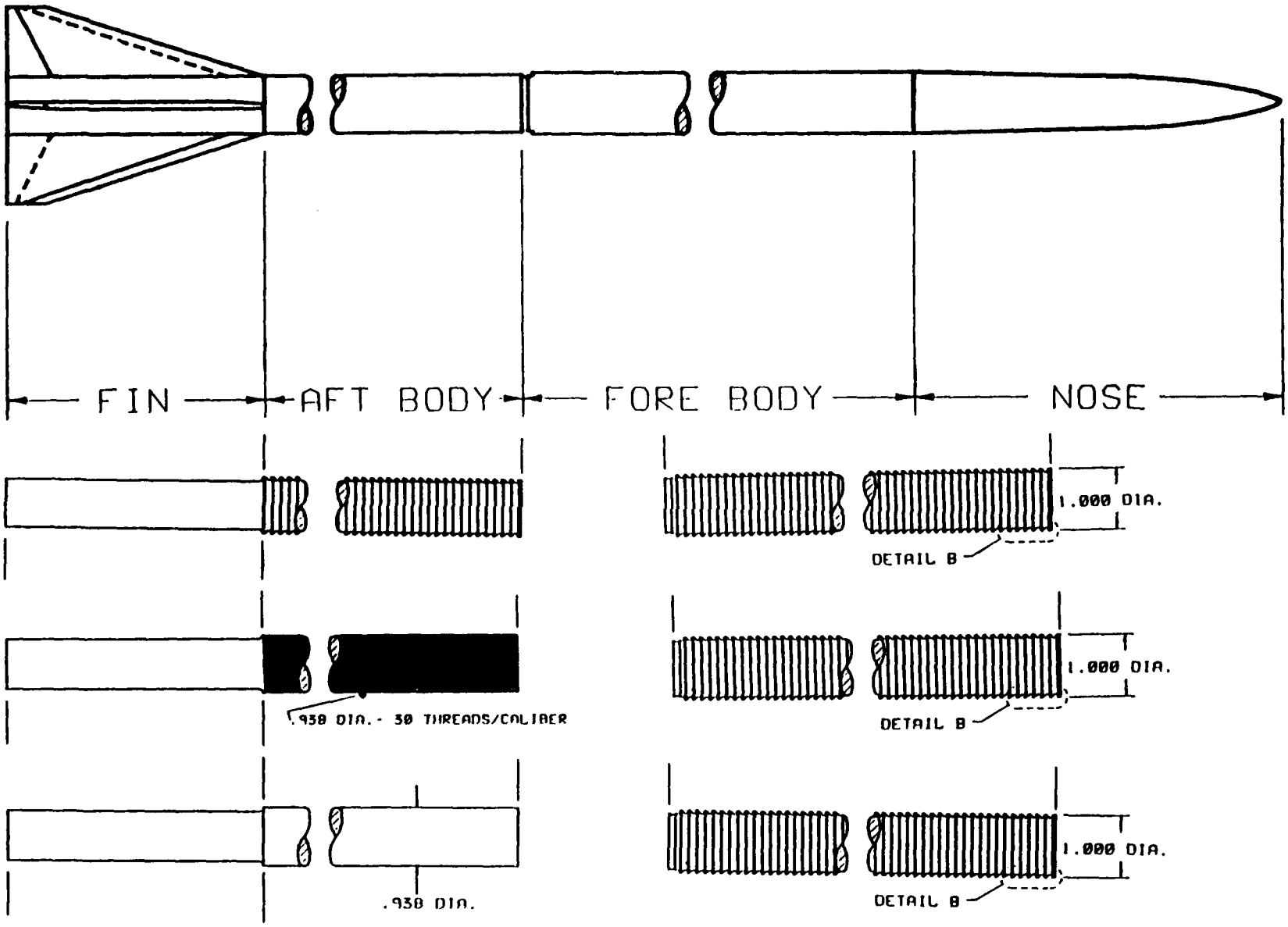

Figure 2. Wind tunnel test model for tests of Reference 1.

a. General configuration.

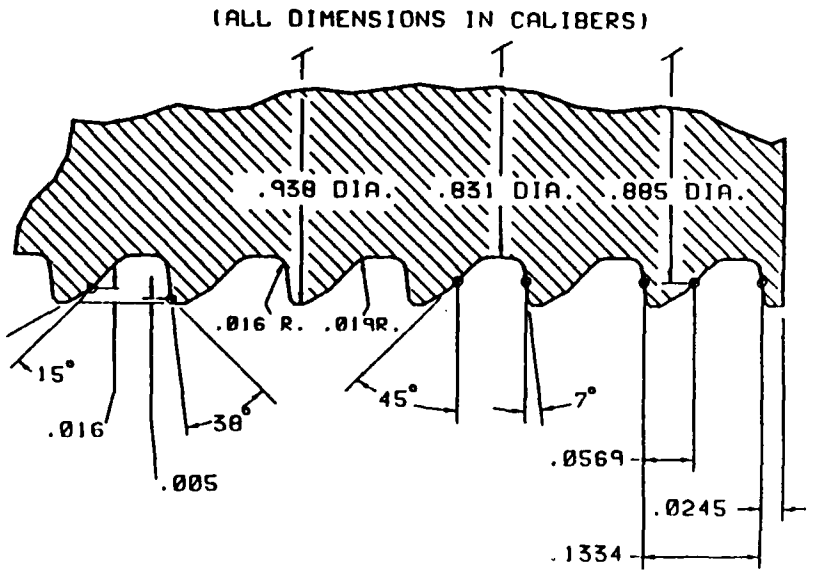

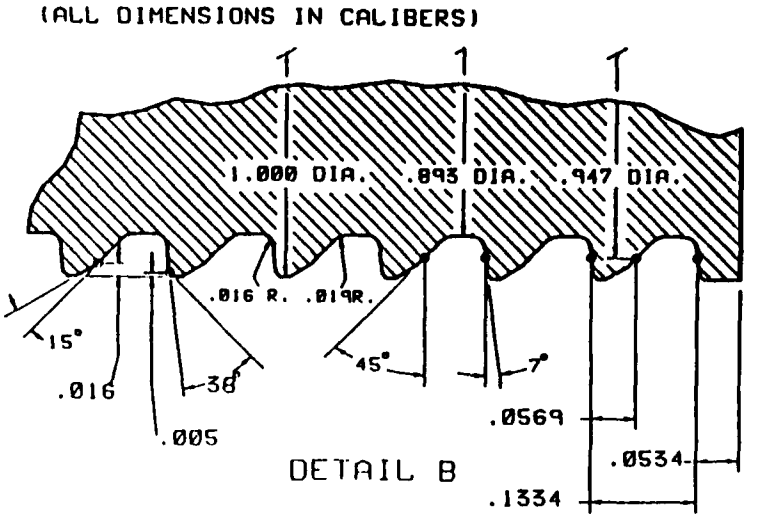

Forebody Groove Detail.

AFTBODY GROOVE DETAIL

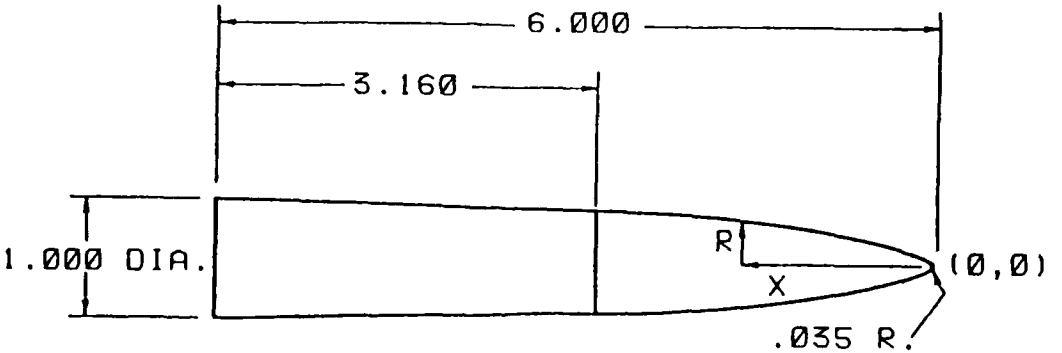

$$R = .432 * (1. - (1. - 2. * X/5.995)^2)^{.75}$$

$$0.0 \leq X \leq 2.839$$

(ALL DIMENSIONS IN CALIBERS)

Sears-Haack nose (Sm SH).

Figure 2. Wind tunnel test model for tests of Reference 1.

b. Nose configuration and grooves geometry.

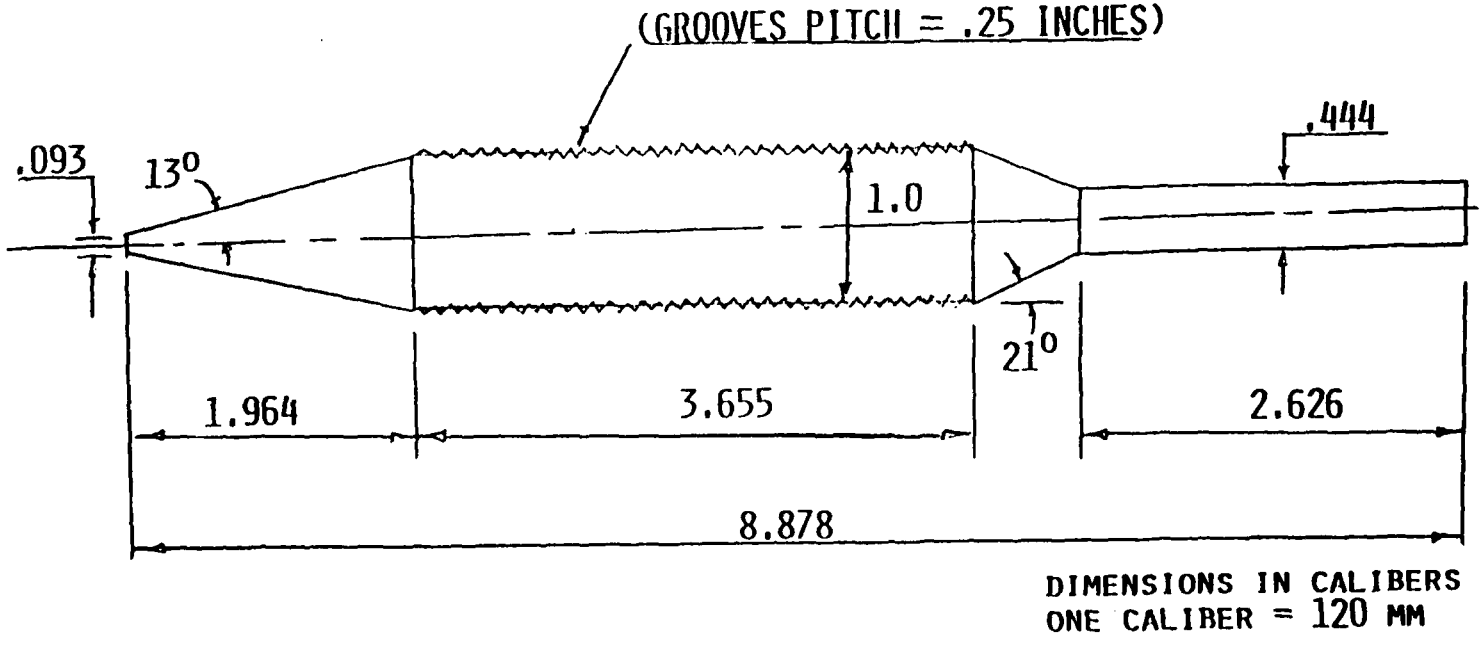

Figure 3. Wind tunnel test model for the tests of Reference 4.

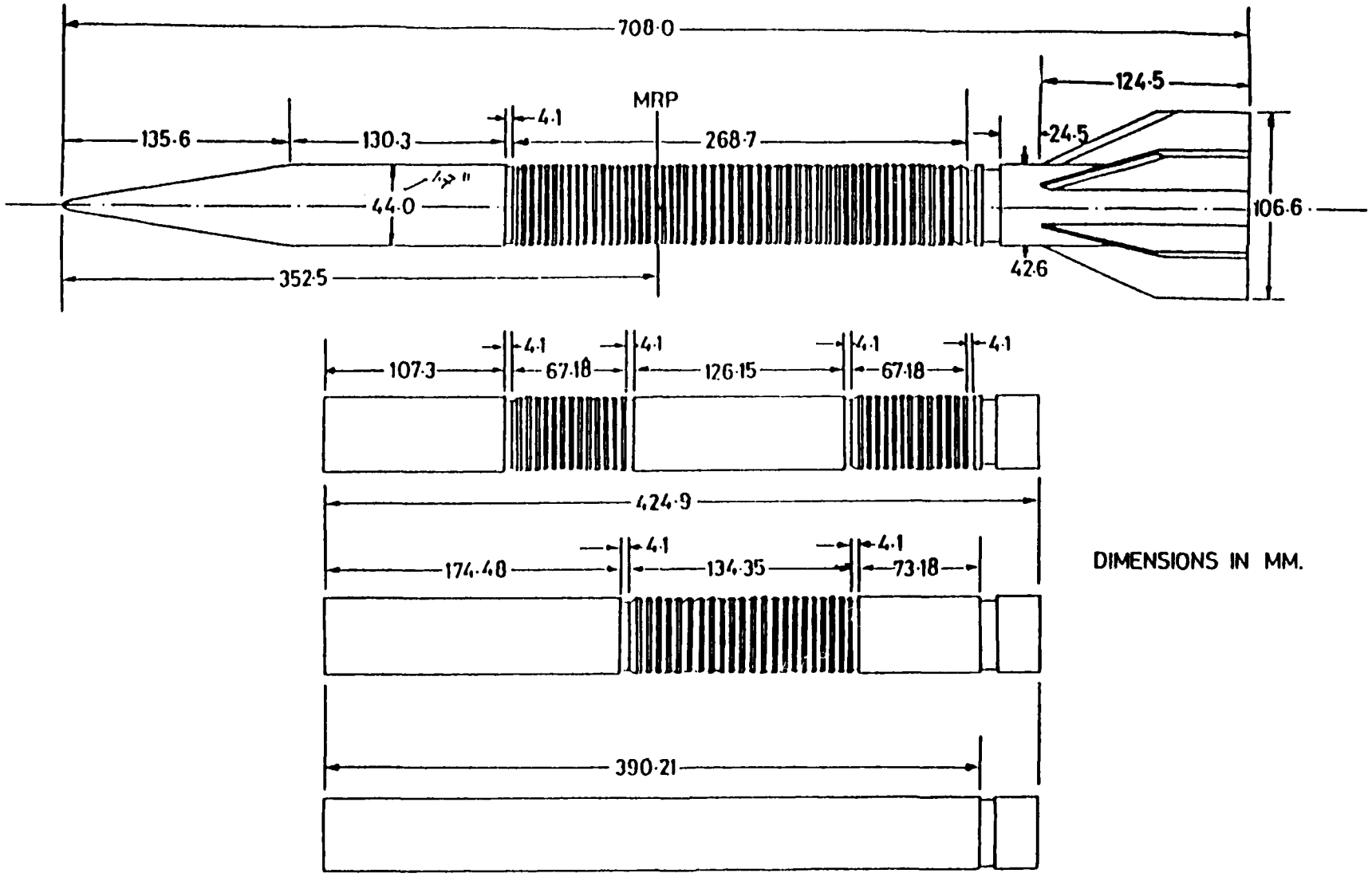

Figure 4. Wind tunnel test model for the tests of Reference 3.

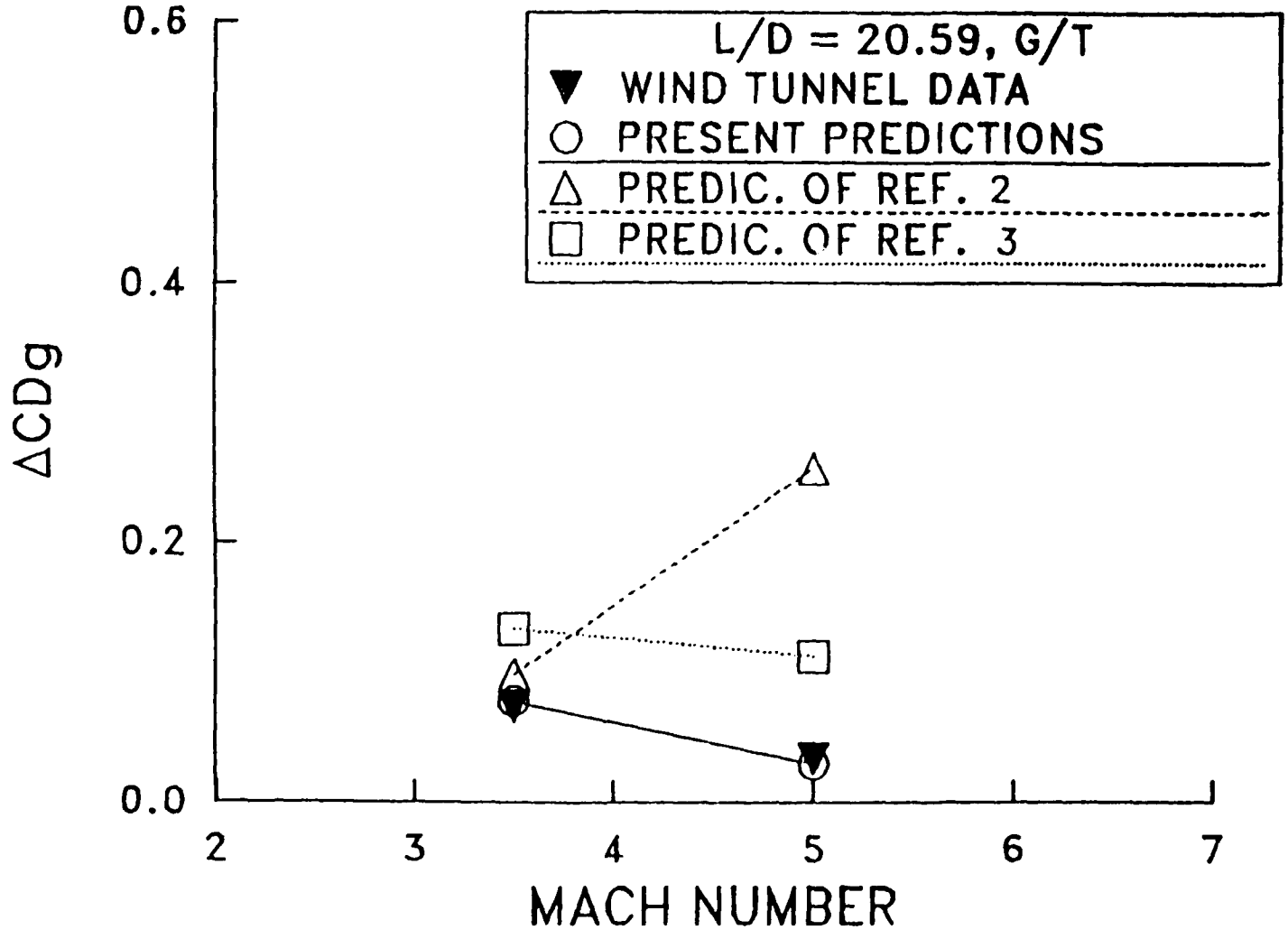

Figure 5. Results of present correlation: validation of ΔC_D with Mach number.

a. For L/D = 20.59.

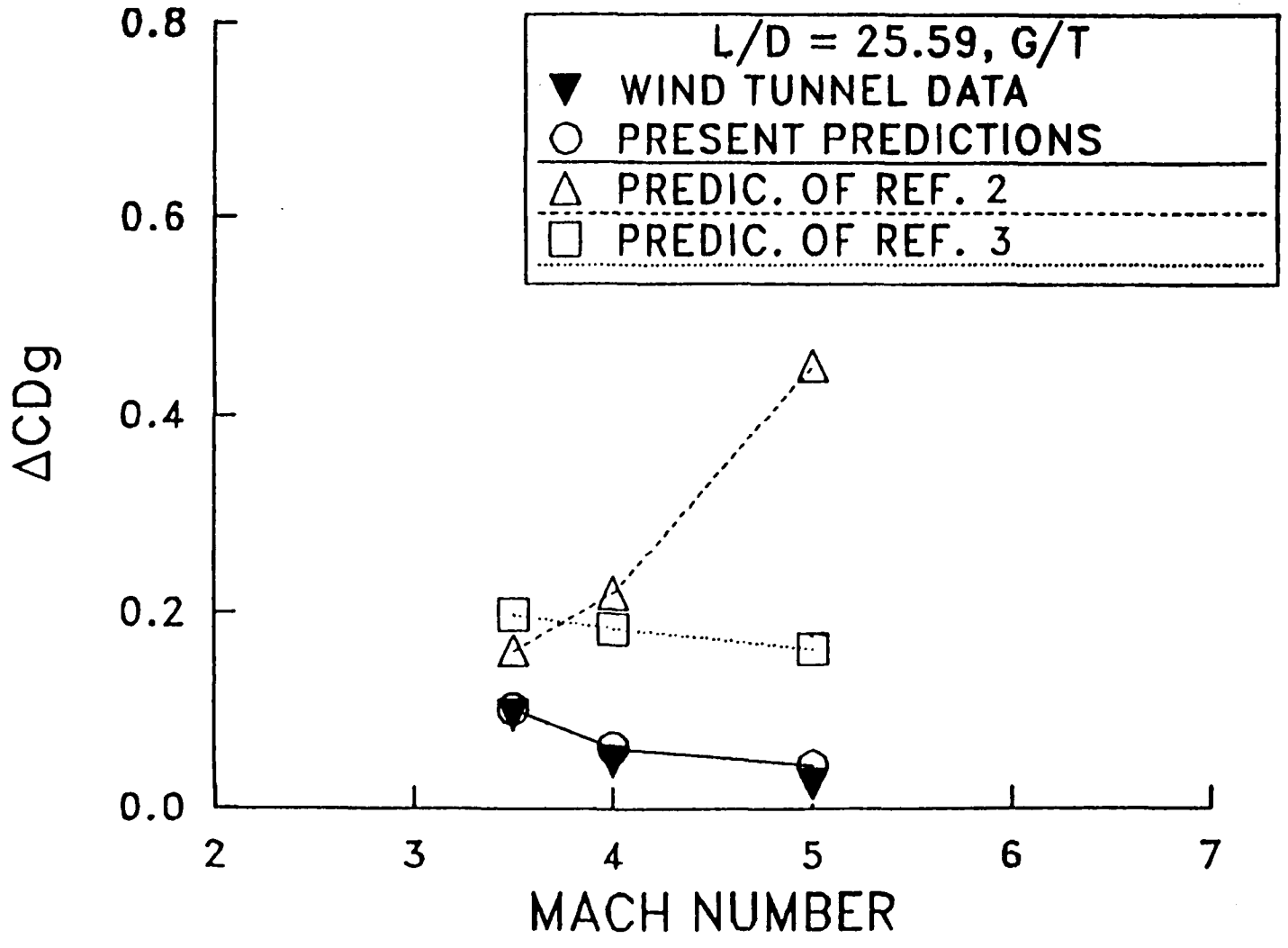

Figure 5. Results of present correlation: validation of ΔC_D with Mach number.

b. For L/D = 25.59.

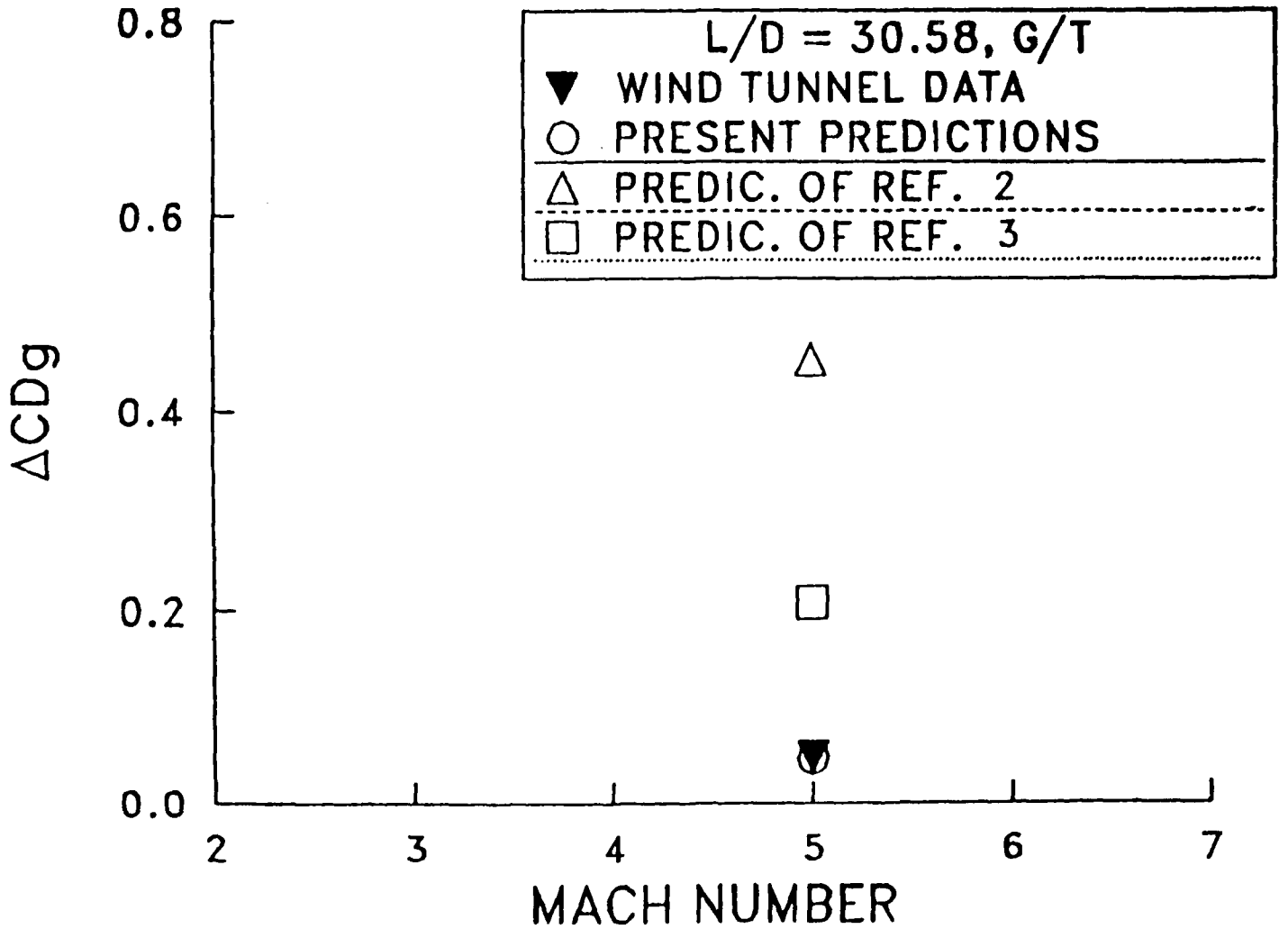

Figure 5. Results of present correlation: validation of ΔC_D with Mach number.

c. For L/D = 30.58.

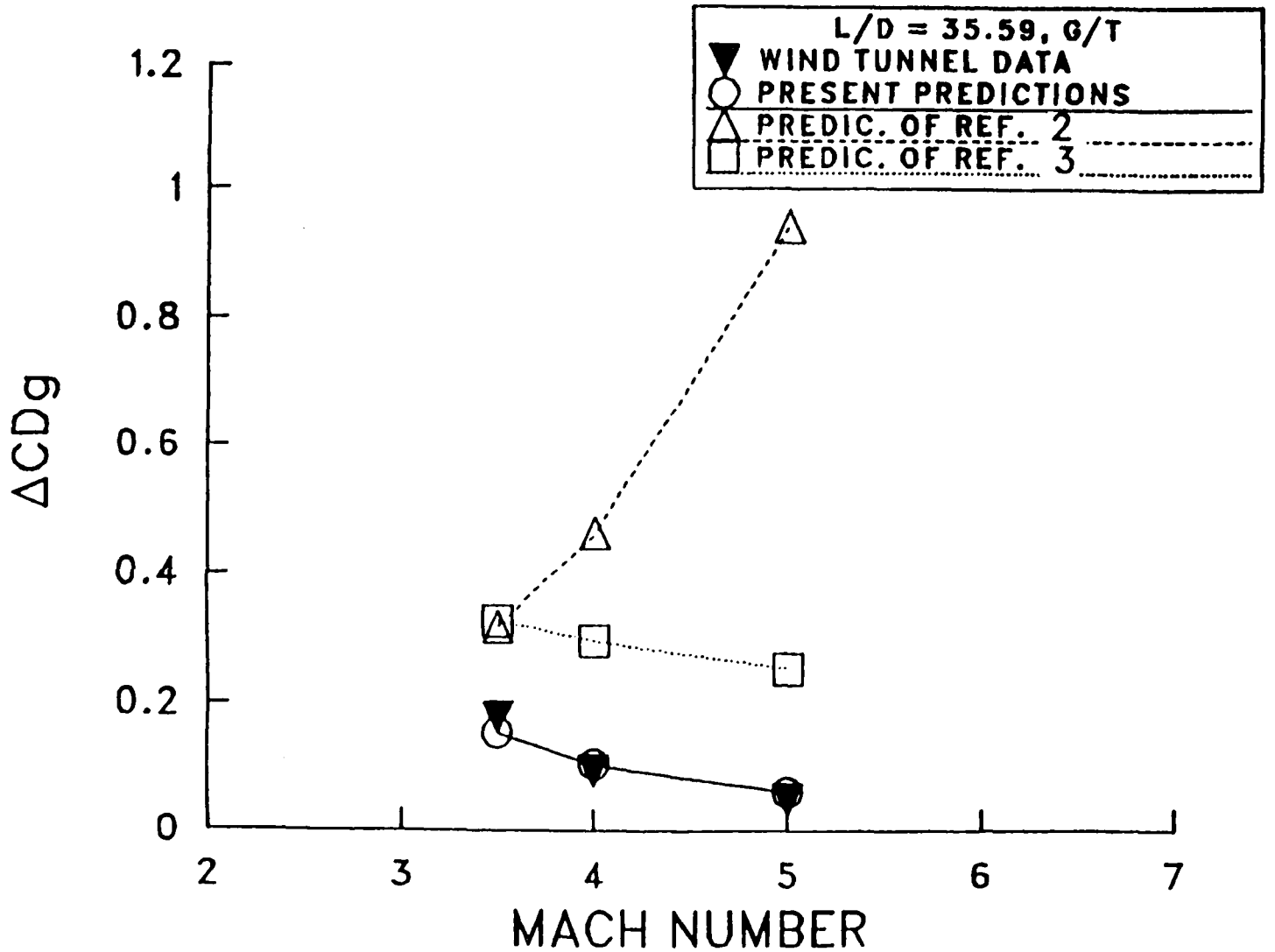

Figure 5. Results of present correlation: validation of ΔC_D with Mach number.

d. For L/D = 35.59.

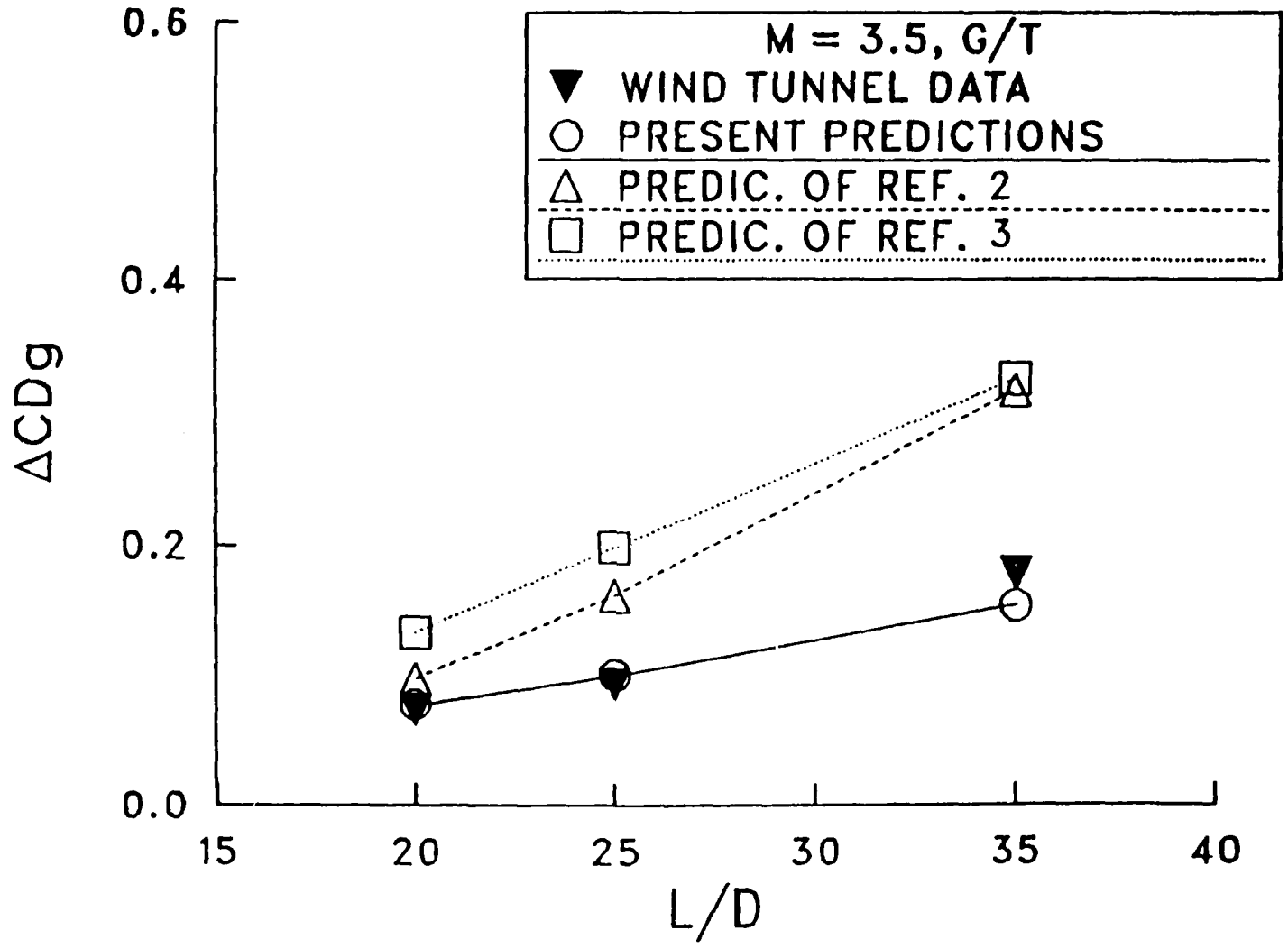

Figure 6. Result of present correlation: variation of ΔC_D with groove length, l_g/D

a. M = 3.5.

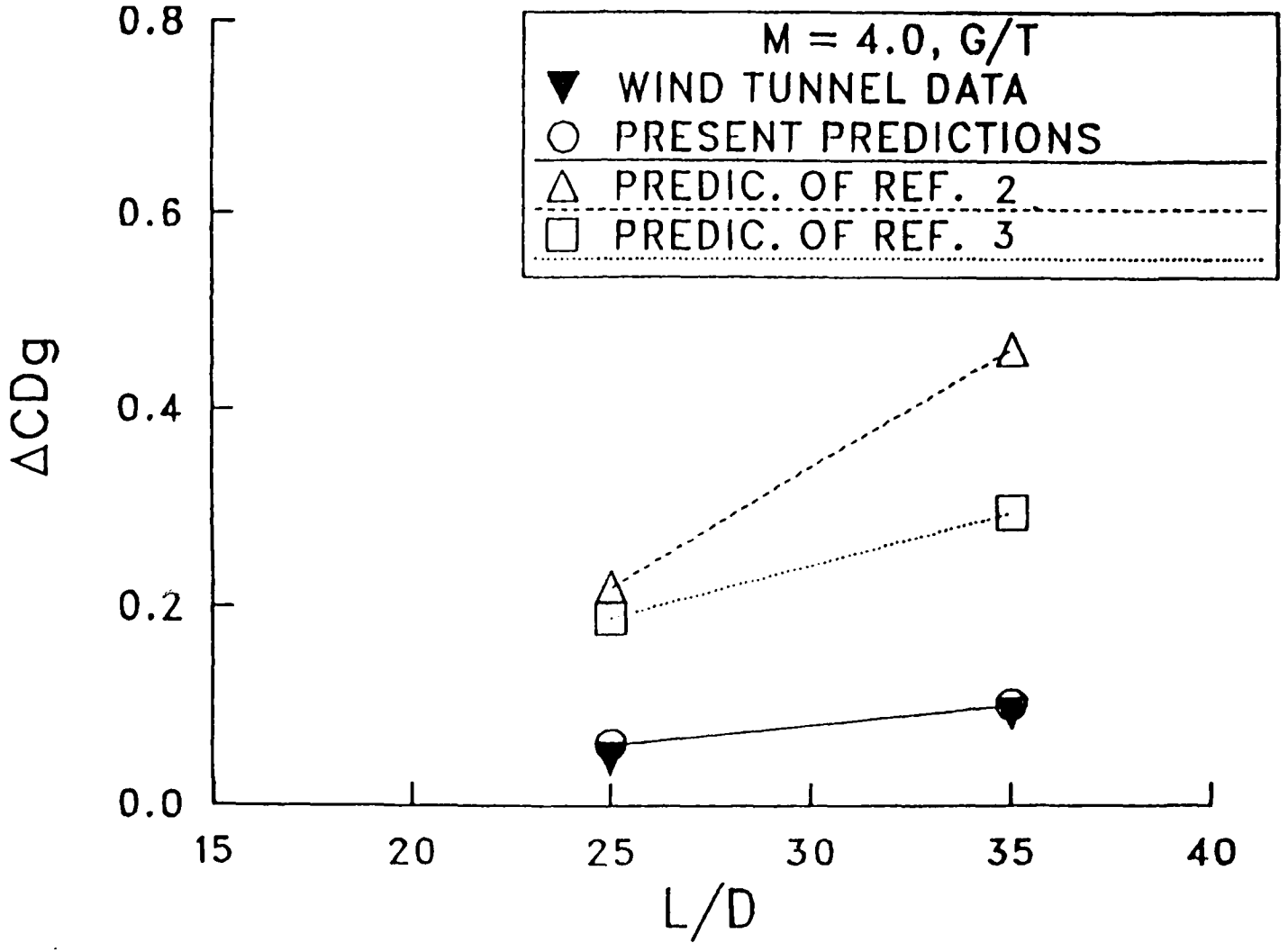

Figure 6. Result of present correlation: variation of ΔC_D with groove length, l_g/D

b. M = 4.0.

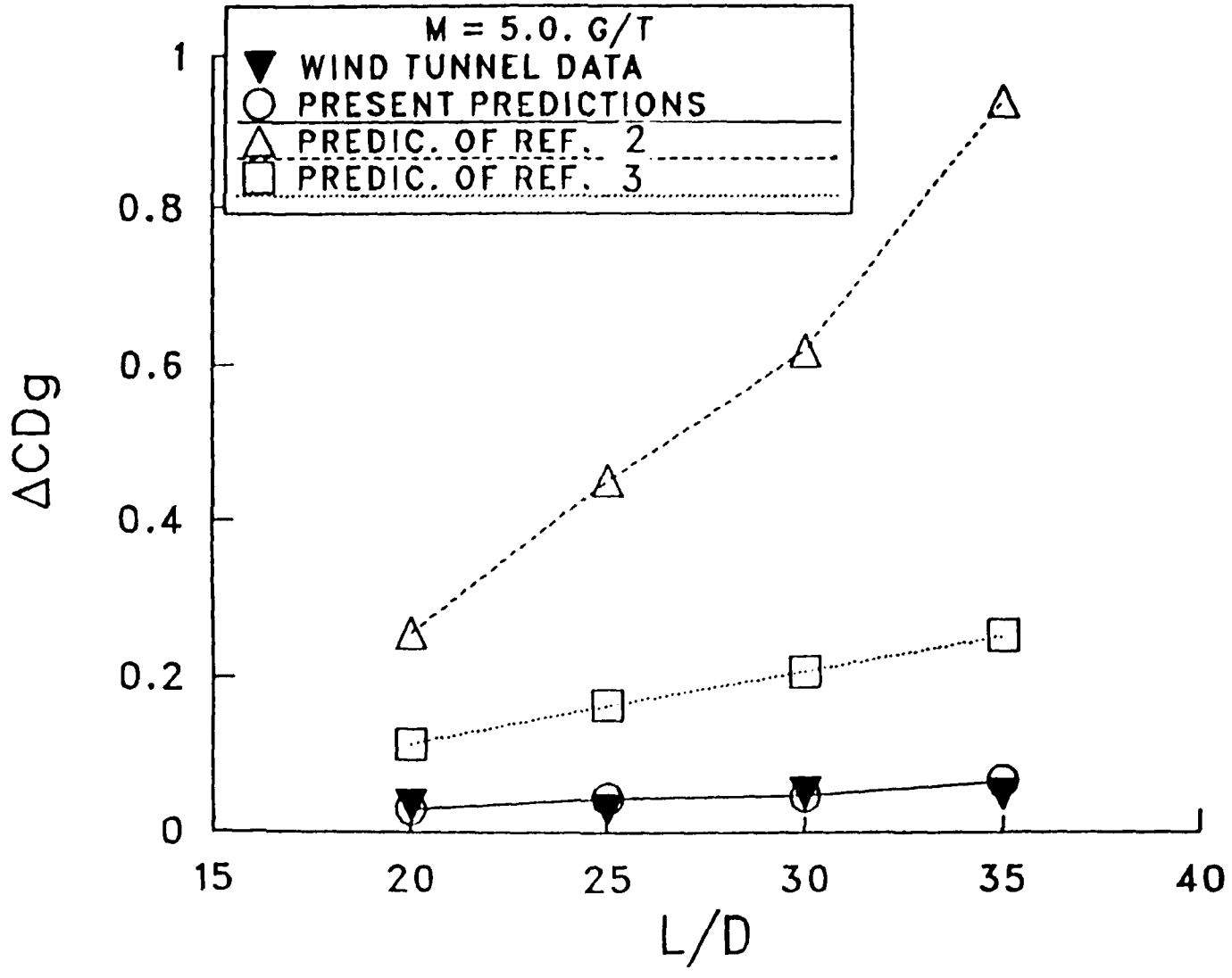

Figure 6. Result of present correlation: variation of ΔC_D with groove length, l_g/D

c. M = 5.0.

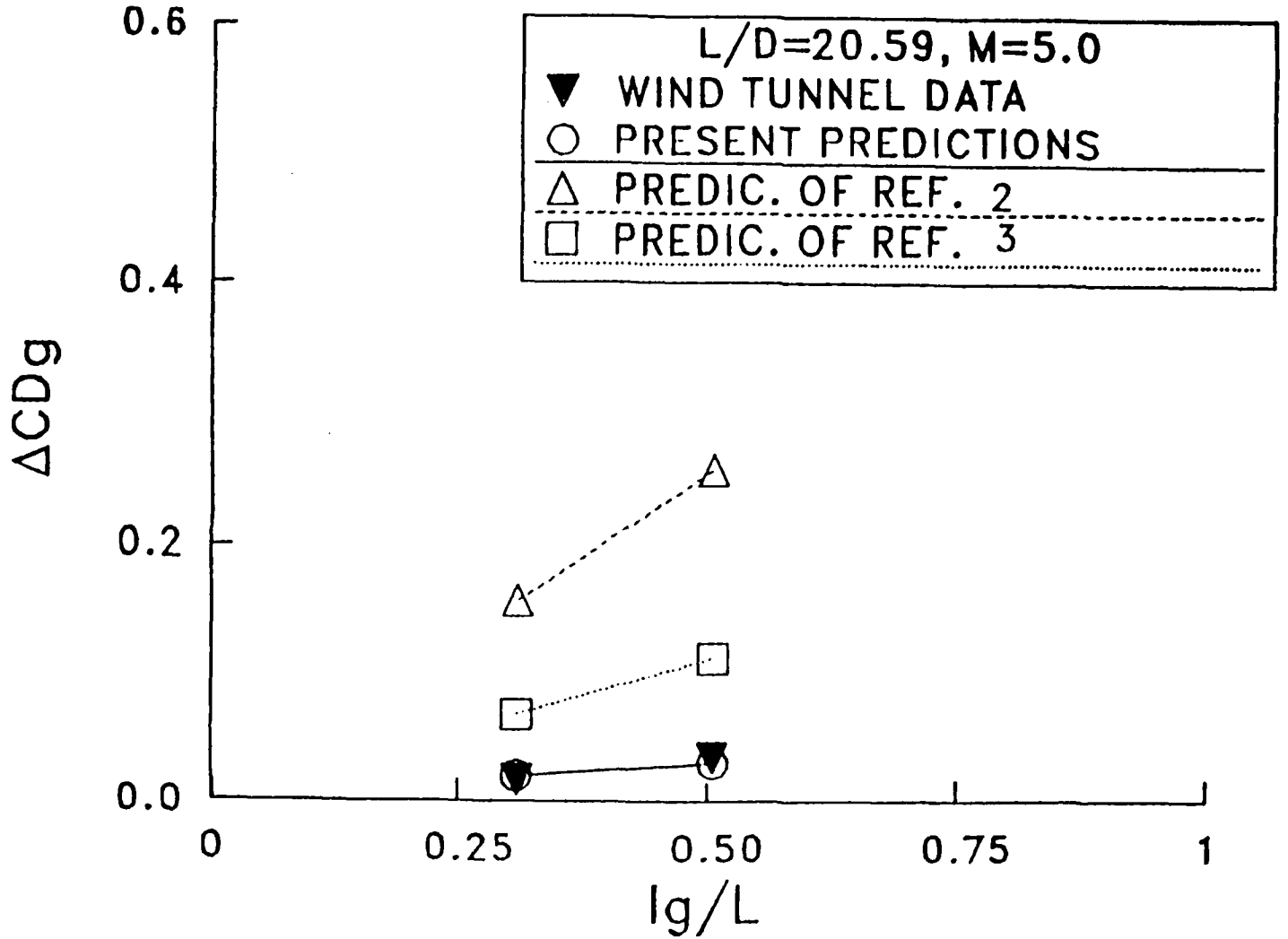

Figure 7. Result of present correlation: variation of ΔC_D with l_g/L.

a. L/D = 20.59, M = 5.0.

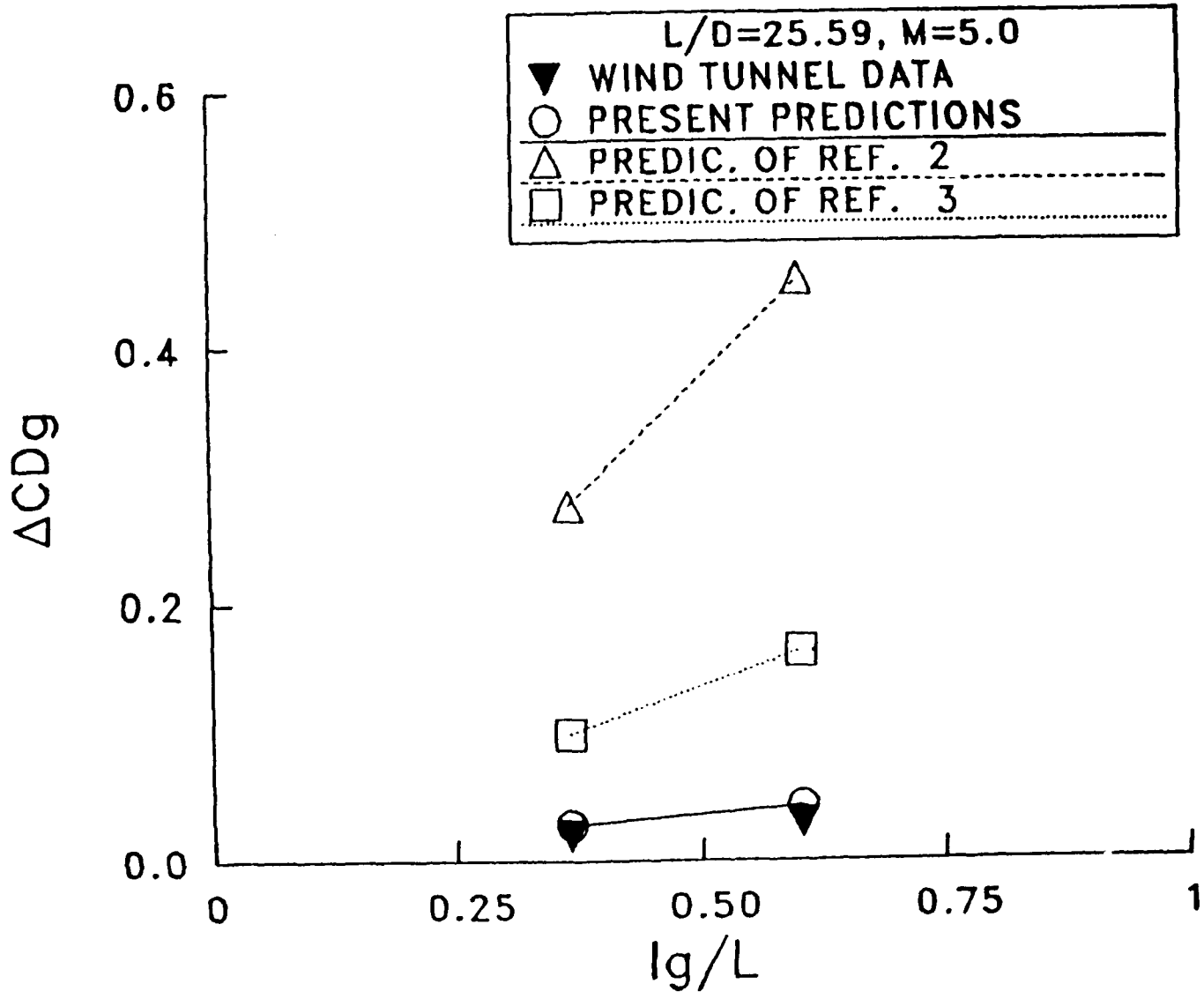

Figure 7. Result of present correlation: variation of ΔC_D with l_g/L.

b. L/D = 25.59, M = 5.0.

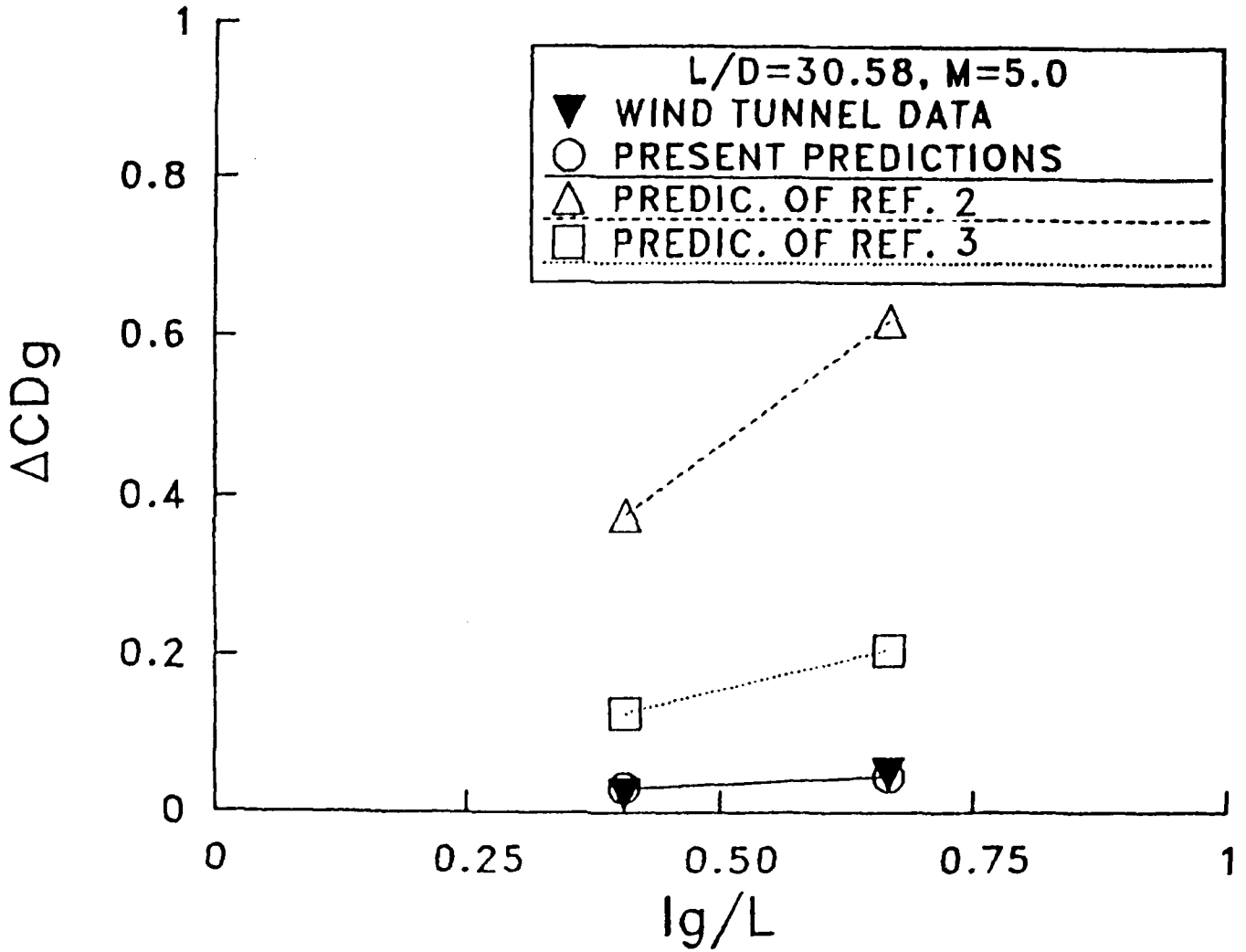

Figure 7. Result of present correlation: variation of ΔC_D with l_g/L.

c. L/D = 30.58, M = 5.0.

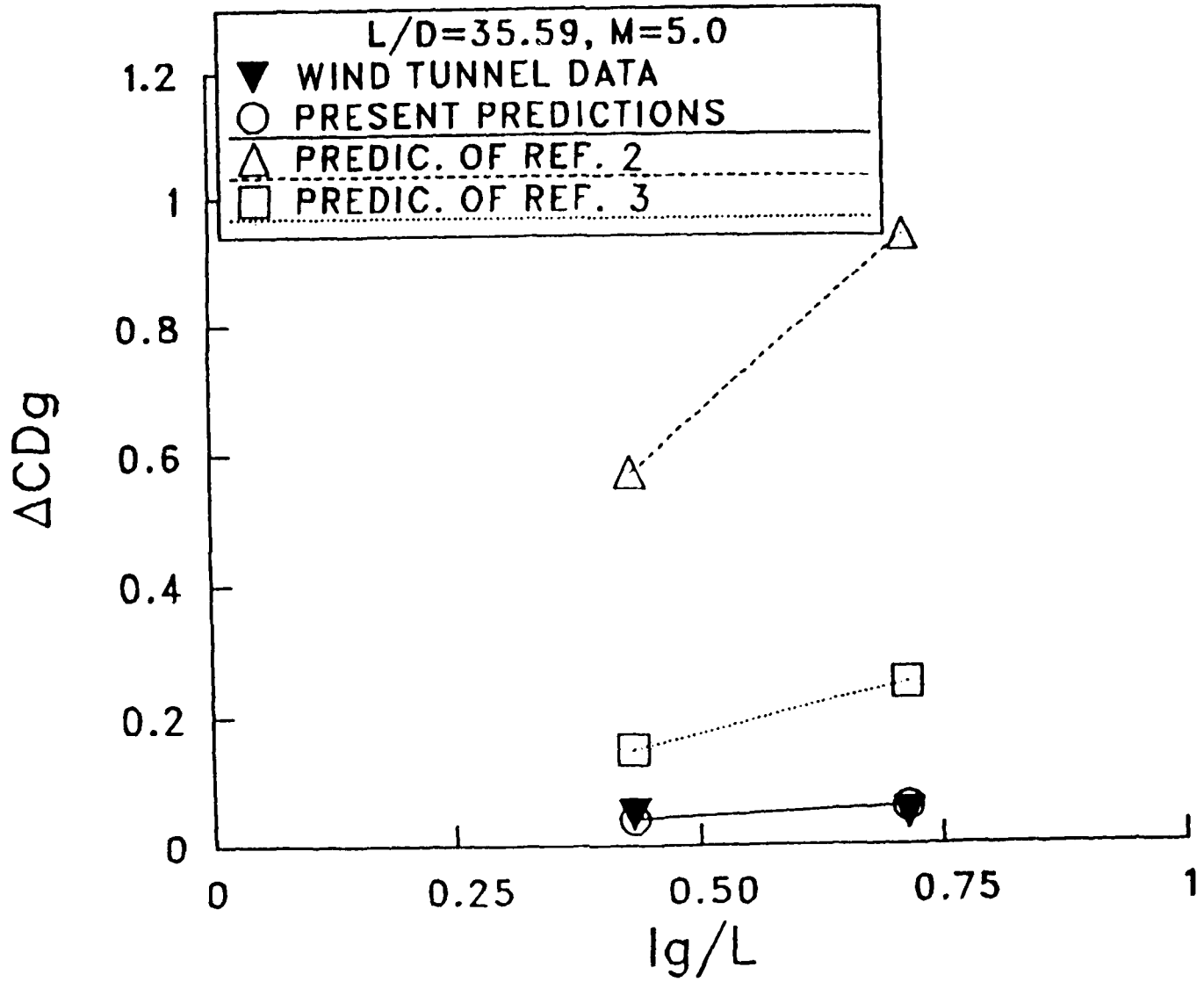

Figure 7. Result of present correlation: variation of ΔC_D with l_g/L.

d. L/D = 35.59, M = 5.0.

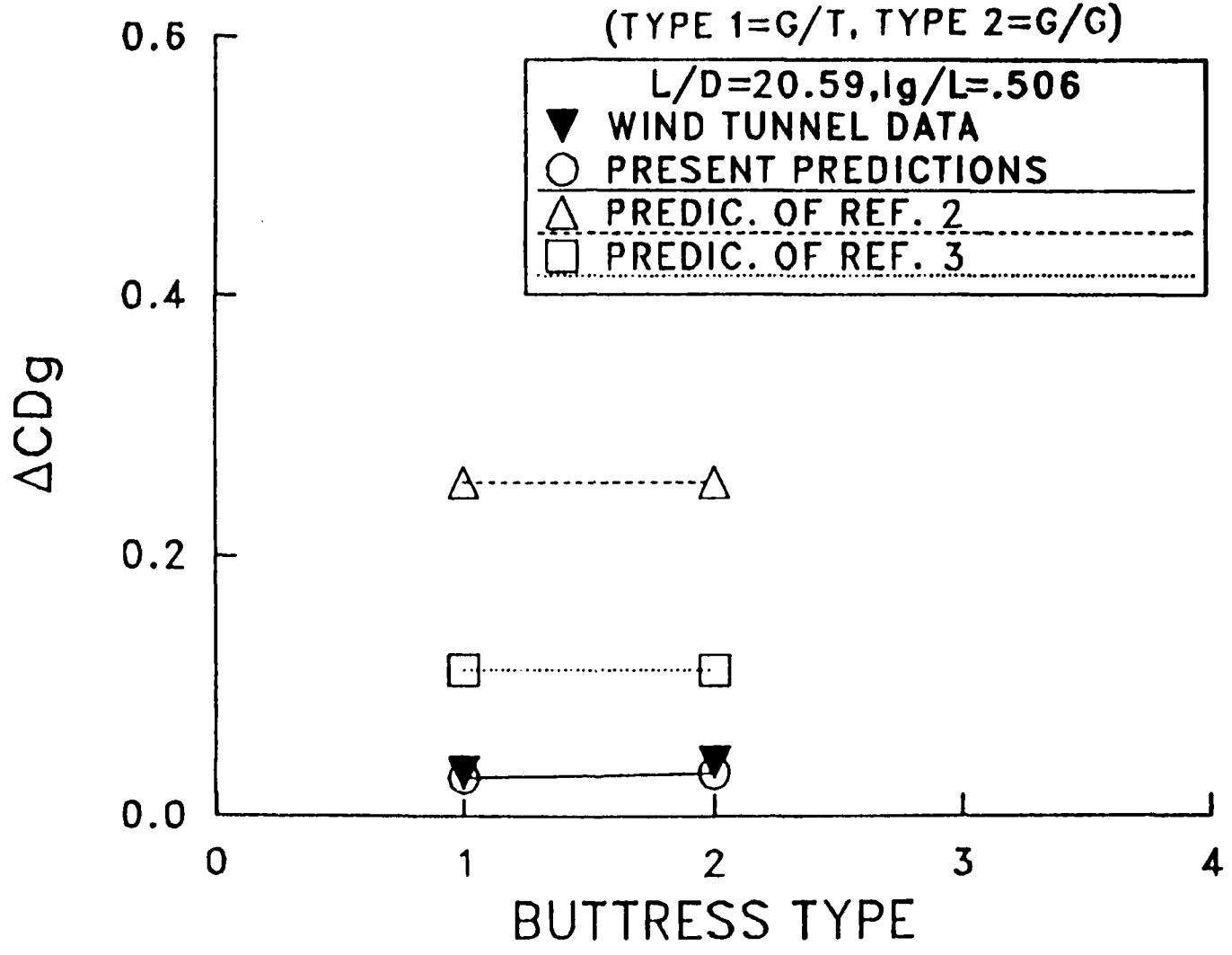

Figure 8. Result of present correlation: variation of ΔC_D with Buttress type.

a. L/D = 20.59, M = 5.0.

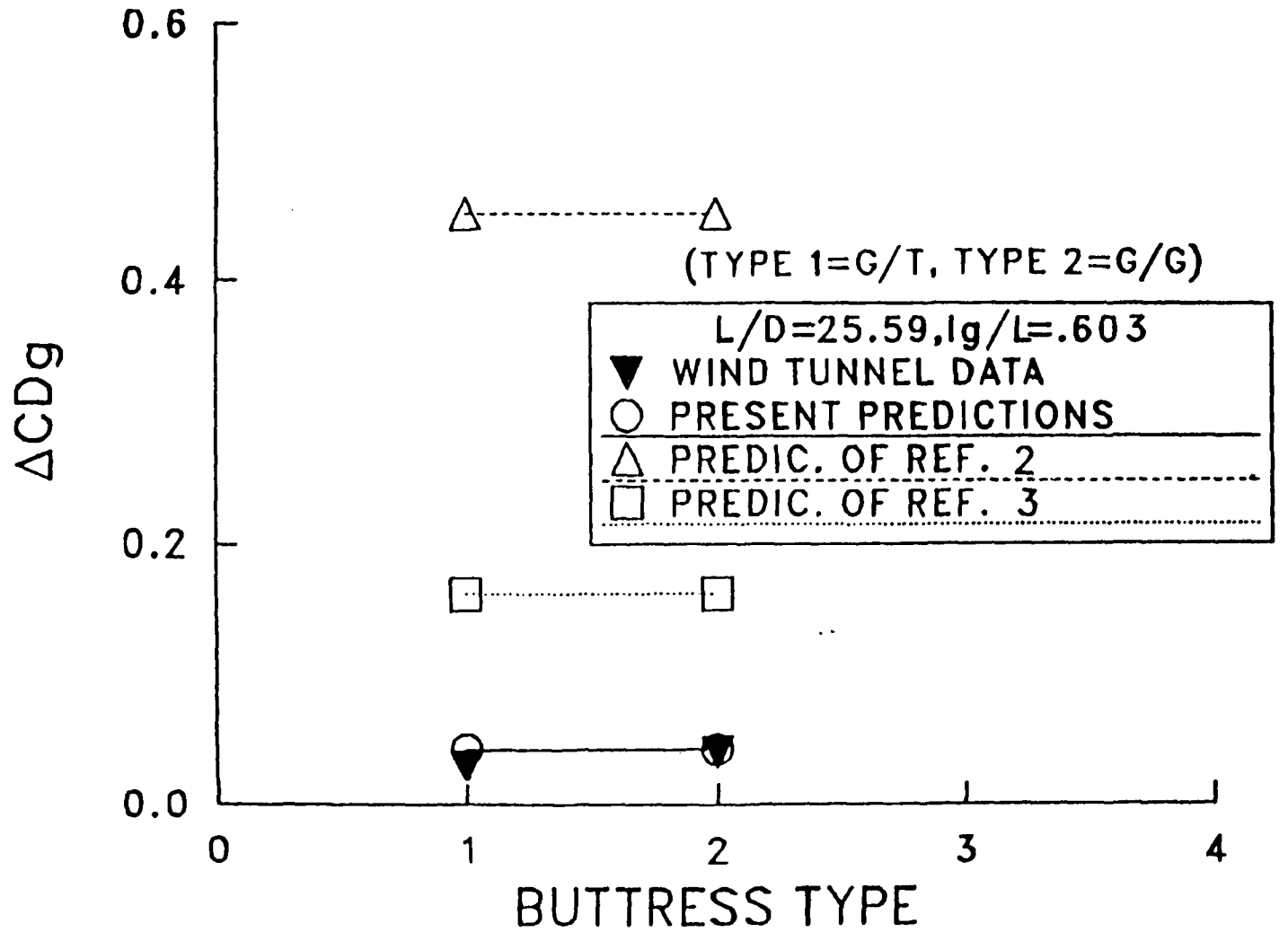

Figure 8. Result of present correlation: variation of ΔC_D with Buttress type.

b. L/D = 25.59, M = 5.0.

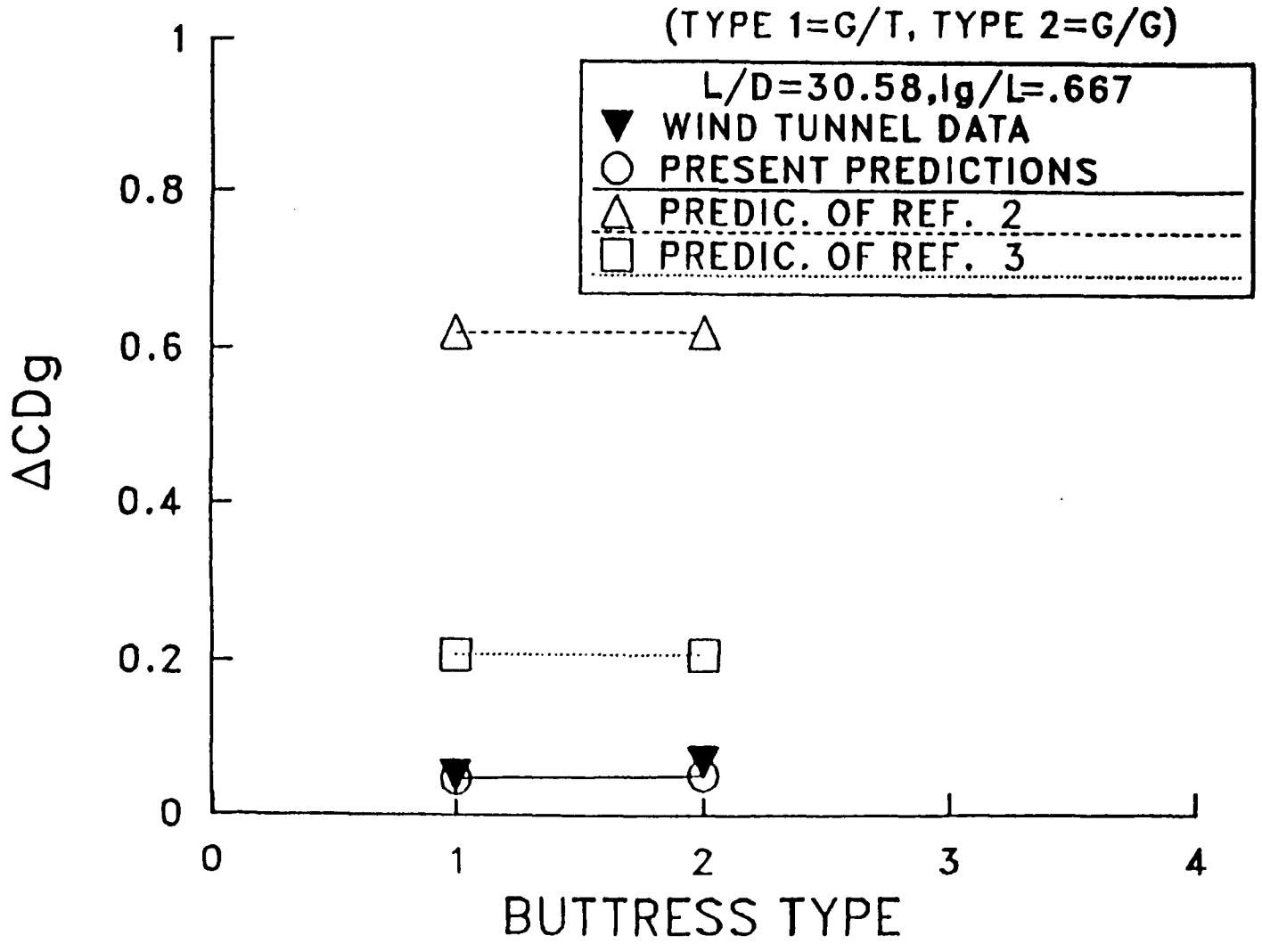

Figure 8. Result of present correlation: variation of ΔC_D with Buttress type.

c. L/D = 30.58, M = 5.0.

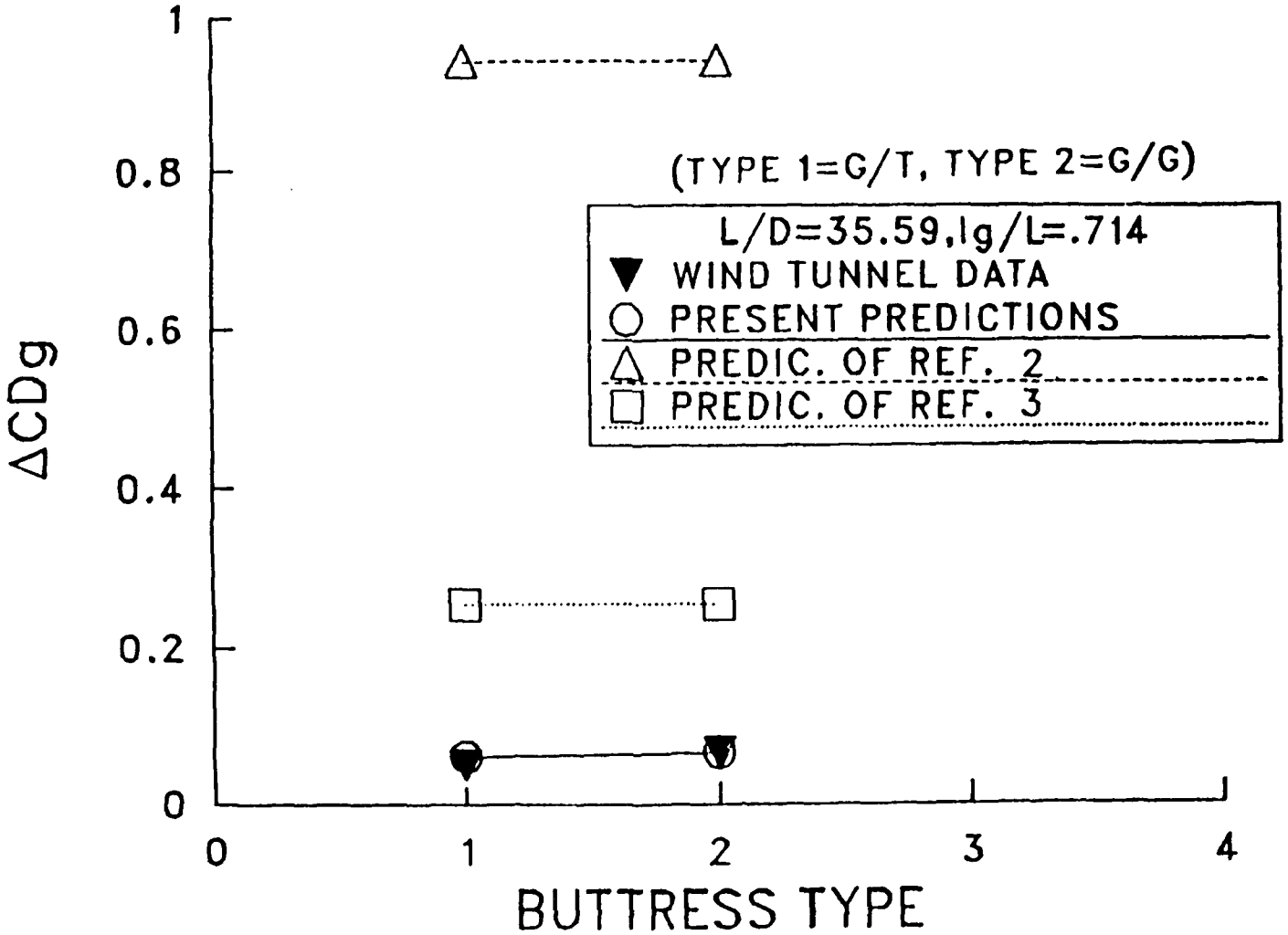

Figure 8. Result of present correlation: variation of ΔC_D with Buttress type.

d. L/D = 35.59, M = 5.0.

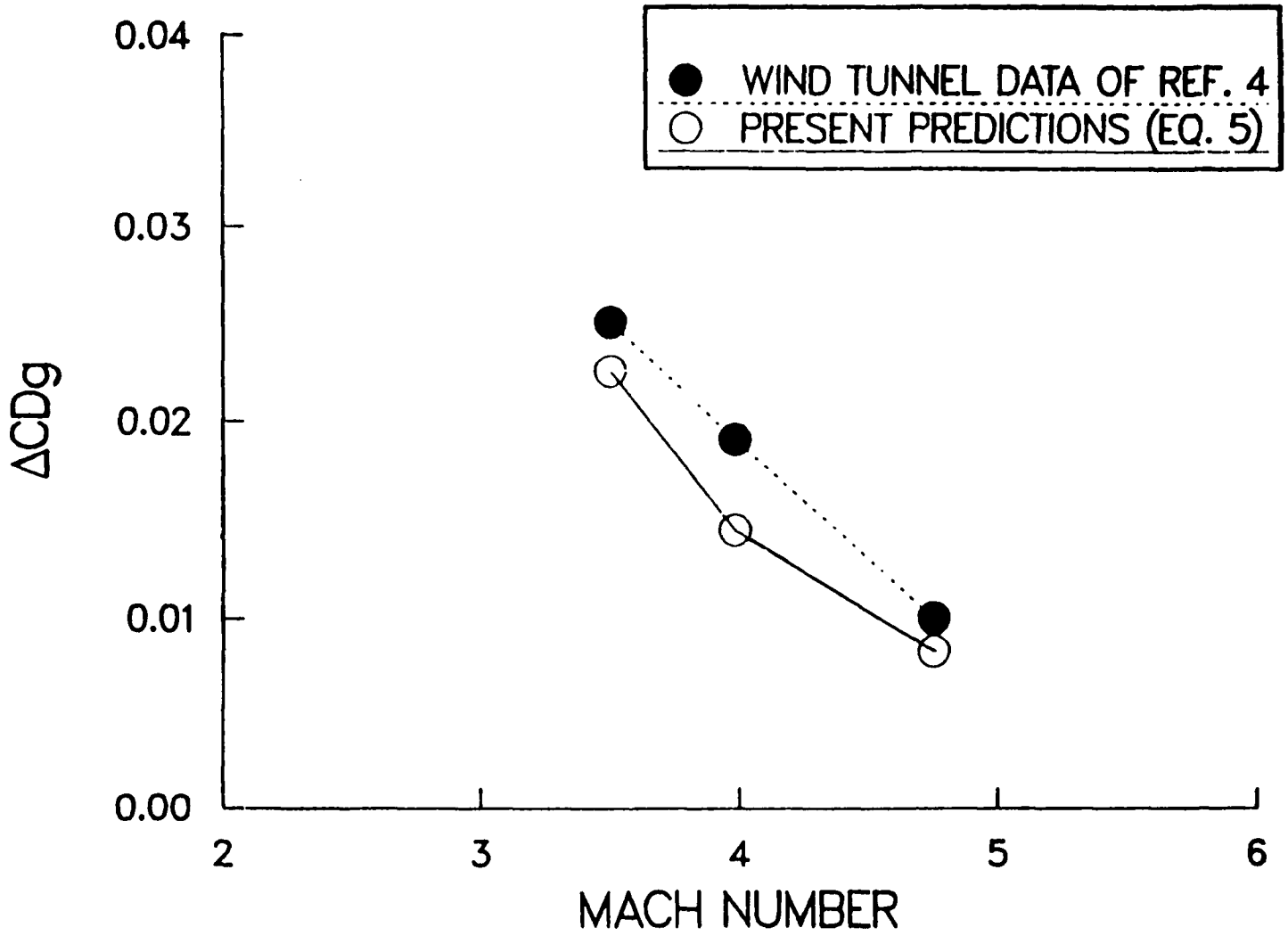

Figure 9. Validation of present predictions against data of Reference 4.

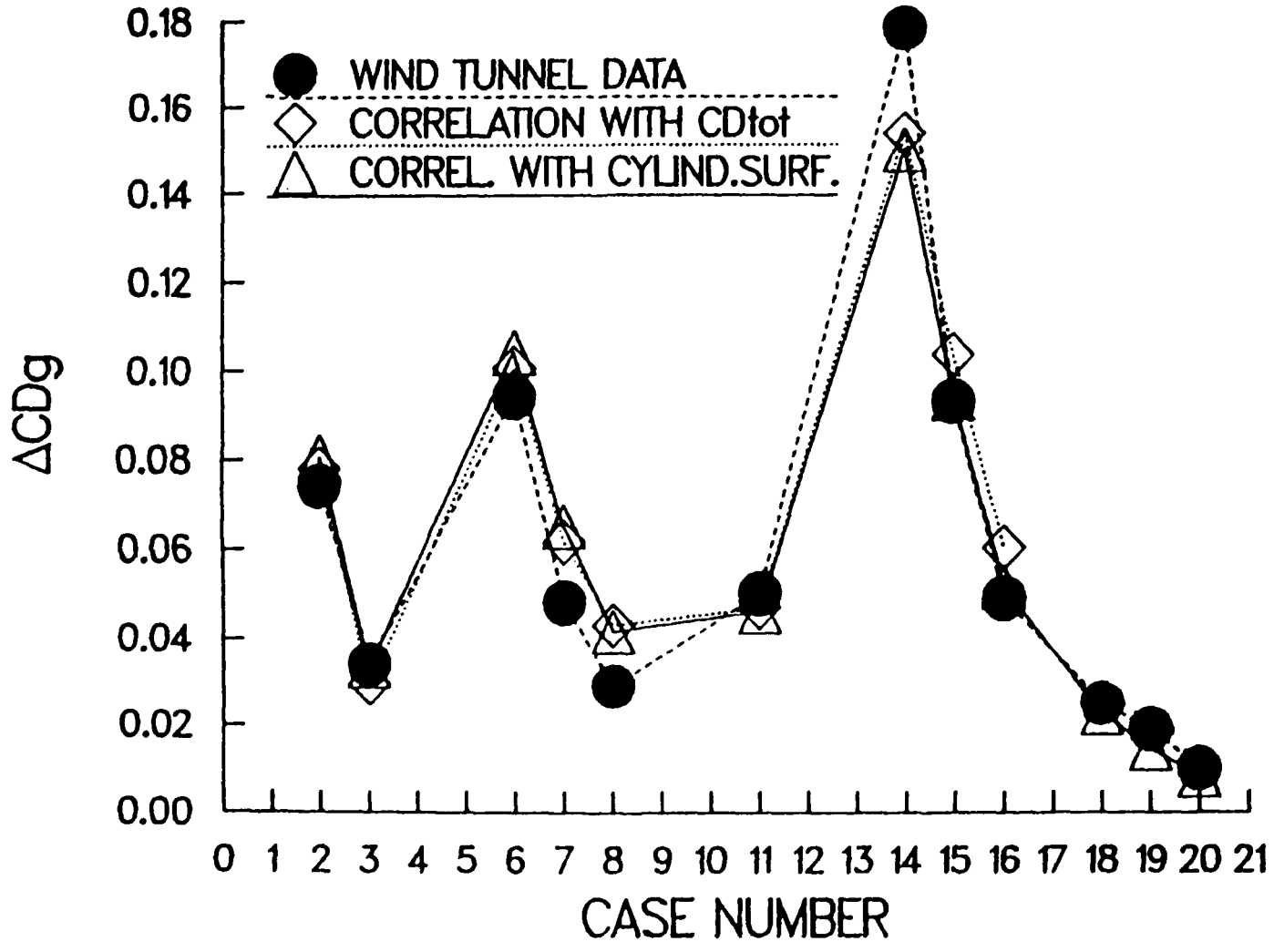

Figure 10. Comparison of the results of the present two correlations.

TABLE 1. Case Designation and Test Conditions of Reference 1.

Case No.	Total length, L (caliber)	Length and Type* of Threads		Cylindrical length, l_c (caliber)	Mach Number	R_e per ft $\times 10^6$	$R_{e_L} \times 10^6$ (based on L)
		l_{g_1} (caliber)	l_{g_2} (caliber)				
1	20.59	6.366(G)	-	10.417	5.0	5.79	9.32
2		6.366(G)	4.051(T)		3.5	4.15	6.68
3		6.366(G)	4.051(T)		5.0	5.65	9.09
4		6.366(G)	4.051(G)		5.0	5.56	8.94
5	25.59	9.392(G)	-	15.420	5.0	5.68	11.36
6		9.392(G)	6.028(T)		3.5	4.19	8.38
7		9.392(G)	6.028(T)		4.0	5.23	10.45
8		9.392(G)	6.028(T)		5.0	5.41	10.81
9		9.392(G)	6.028(G)		5.0	5.88	11.76
10	30.58	12.408(G)	-	20.412	5.0	5.71	13.65
11		12.408(G)	8.004(T)		5.0	5.71	13.64
12		12.408(G)	8.004(G)		5.0	5.76	13.77
13	35.59	15.424(G)	-	25.420	5.0	5.65	15.72
14		15.424(G)	9.996(T)		3.5	3.79	10.55
15		15.424(G)	9.996(T)		4.0	4.49	12.48
16		15.424(G)	9.996(T)		5.0	5.70	15.83
17		15.424(G)	9.996(G)		5.0	5.81	16.15

* TYPE: (G) for grooves (8 grooves per inch)
(T) for threads (32 threads per inch)

TABLE 2. Case Designation and Test Conditions of Reference 4.

Case No.	Mach Number	R_e per ft $\times 10^{-6}$	C_D Wind Tunnel		ΔC_{D_g} Wind Tunnel
			Grooved Body	Smooth Body	
18	3.49	12	0.280	0.255	0.025
19	3.98	14	0.227	0.208	0.019
20	4.75	18	0.196	0.186	0.010

TABLE 3. Comparison of Present Predictions with Data of References 1 and 4.

Case No.	C_D Wind Tunnel		ΔC_{D_g}	
	Grooved Body	Smooth Body	Wind Tunnel	Present Predictions Eq. (3)
1	0.213	0.197	0.016	0.0193
2	0.384	0.310	0.074	0.0779
3	0.231	0.197	0.034	0.0294
4	0.238	0.197	0.041	0.0331
5	0.256	0.236	0.020	0.0275
6	0.434	0.340	0.094	0.1005
7	0.328	0.280	0.048	0.0615
8	0.265	0.236	0.029	0.0429
9	0.277	0.236	0.041	0.0434
10	0.282	0.258	0.024	0.0312
11	0.308	0.258	0.050	0.0469
12	0.327	0.258	0.069	0.0509
13	0.298	0.248	0.050	0.0407
14	0.578	0.400	0.178	0.1532
15	0.450	0.357	0.093	0.1035
16	0.347	0.297	0.049	0.0603
17	0.354	0.298	0.056	0.0656
18	0.280	0.255	0.025	Not Applicable
19	0.227	0.208	0.019	
20	0.196	0.186	0.010	

TABLE 4. Comparison of the Present Two Correlations.

Case No.	ΔC_{D_g}		
	Wind Tunnel	Present Predictions Eq. (3)	Present Predictions Eq. (5)
2	0.074	0.0779	0.0805
3	0.034	0.0294	0.0334
6	0.094	0.1005	0.1040
7	0.048	0.0615	0.0650
8	0.029	0.0429	0.0415
11	0.050	0.0469	0.0461
14	0.178	0.1532	0.1494
15	0.093	0.1035	0.0937
16	0.049	0.0603	0.0514
18	0.025	Not Applicable	0.0226
19	0.019		0.0144
20	0.010		0.0083

REFERENCES

1. Brandon, F. and Von Wahlde, R., "Wind Tunnel Data for Long-Rod Fin-Stabilized Projectiles," BRL-MR-3618, US Army Ballistic Research Laboratory, Aberdeen Proving Ground, Maryland, July 1987.

2. Donovan, W.F., Nusca, M.J., and Woods, S., "Automatic Plotting Routines for Estimating Static Aerodynamic Properties of Long Rod Finned Projectiles for $2 < M < 5$," ARBRL-MR-03123, US Army Ballistic Research Laboratory, Aberdeen Proving Ground, Maryland, August 1981.

3. Hendry, C.E., "Contract MW 22B/807 - Aerodynamics of Long Projectiles - Final Report, Part 2," British Aerospace PLC, Dynamics Group, Sowerby Research Center, Bristol, U.K., Report No. JS 10134, August 1984.

4. Meissner, R. and Malinoski, F., unpublished wind tunnel data, US Army Ballistic Research Laboratory, Aberdeen Proving Ground, Maryland, August 1987.

5. McCoy, R.L., "'McDRAG' - A Computer Program for Estimating the Drag Coefficient of Projectiles," ARBRL-TR-02293, US Army Ballistic Research Laboratory, Aberdeen Proving Ground, Maryland, February 1981. (AD A098110)

6. Mikhail, A.G., "Fin Gaps and Body Slots: Effects and Modeling for Guided Projectiles," BRL-TR-2808, US Army Ballistic Research Laboratory, Aberdeen Proving Ground, Maryland, June 1987. (Also, Journal of Spacecraft and Rockets, Vol. 25, No. 5, September-October 1988, pp. 345-353, and AIAA Paper No. 87-0447, January 1987.)

7. Gai, S.L. and Patil, S.R., "Subsonic Axisymmetric Base Flow Experiments with Base Modifications," Journal of Spacecraft and Rockets, Vol. 17, No. 1, January-February 1980, pp. 42-46.

LIST OF SYMBOLS

A_{ref} = projectile reference area, $(\pi D^2/4)$

C_A = axial force coefficient

C_D = drag coefficient, drag force/$(0.5\rho_\infty V^2 A_{ref})$

$C_{D_{TSB}}$ = body-alone total drag coefficient (including base drag) for for the smooth body (i.e., without grooves) configuration

$C_{D_{SFSB}}$ = drag coefficient due to skin friction of the smooth body of the cylindrical portion, l_c, of the body

c_f = skin friction coefficient

d_c = diameter of the cylindrical portion, in calibers

D = reference diameter of the projectile

h = groove depth

KE = kinetic energy

l_c = length of the cylindrical portion of the body, in calibers

l_g, l_{g_1}, l_{g_2} = axial length of the grooved portion of the projectile body

L = reference length of the projectile, usually the total length except as otherwise noted

M = projectile Mach number

p = groove pitch

R_e = Reynolds number per unit length

R_{e_L} = Reynolds number based on the total length of the projectile

V = projectile velocity

x_o = distance from the nose tip to the first groove

Greek Symbols

α = angle of attack

ρ_∞ = free stream air density

τ = shear stress at the wall

DISTRIBUTION LIST

No. of Copies	Organization
12	Administrator Defense Technical Info Center ATTN: DTIC-DDA Cameron Station Alexandria, VA 22304-6145
1	HQDA (SARD-TR) Washington, DC 20310-0001
1	Commander US Army Materiel Command ATTN: AMCDRA-ST 5001 Eisenhower Avenue Alexandria, VA 22333-0001
1	Commander US Army Laboratory Command ATTN: AMSLC-DL Adelphi, MD 20783-1145
2	Commander Armament RD&E Center US Army AMCCOM ATTN: SMCAR-MSI Picatinny Arsenal, NJ 07806-5000
2	Commander Armament RD&E Center US Army AMCCOM ATTN: SMCAR-TDC Picatinny Arsenal, NJ 07806-5000
4	Commander US Army Armament Research, Development and Engineering Center ATTN: SMCAR-LCA-F/R. Kline S. Kahn H. Hudgins J. Grau Dover, NJ 07801-5001
1	Director Benet Weapons Laboratory Armament RD&E Center US Army AMCCOM ATTN: SMCAR-LCB-TL Watervliet, NY 12189-4050
1	Commander US Army Armament, Munitions and Chemical Command ATTN: SMCAR-ESP-L Rock Island, IL 61299-5000
1	Commander US Army Aviation Systems Command ATTN: AMSAV-DACL 4300 Goodfellow Blvd. St. Louis, MO 63120-1798
1	Director US Army Aviation Research and Technology Activity Ames Research Center Moffett Field, CA 94035-1099
1	Commander US Army Missile Command ATTN: AMSMI-AS Redstone Arsenal, AL 35898-5010
1	Commander US Army Tank Automotive Command ATTN: ASQNC-TAC-DI (Technical Library) Warren, MI 48397-5000
1	Director US Army TRADOC Analysis Center ATTN: ATAA-SL White Sands Missile Range, NM 88002-5502
1	Director Combat Development ATTN: ATSH-CD-CSO-OR Fort Benning, GA 31905-5660

DISTRIBUTION LIST

No. of Copies	Organization
1	AFWL/SUL Kirtland AFB, NM 87117-5800
1	Air Force Armament Laboratory ATTN: AFATL/DLODL Eglin AFB, FL 32542-5000
2	Commander US Naval Surface Weapons Center ATTN: Dr. F. Moore Dr. T. Clare, Code DK20 Dahlgren, VA 22448
1	Commander US Naval Surface Weapons Center ATTN: Dr. A. Wardlaw Silver Spring, MD 20910
2	Sandia Laboratories ATTN: Dr. W.L. Oberkampf Dr. F. Blottner Division 1636 Sandia National Laboratories Albuquerque, NM 87185
1	Director NASA Ames Research Center ATTN: MS-227-8, L. Schiff Moffett Field, CA 94035
1	Director Defense Advanced Research Projects Agency ATTN: Tactical Technology Office 1400 Wilson Boulevard Arlington, VA 22209
1	Massachusetts Institute of Technology ATTN: Tech Library 77 Massachusetts Avenue Cambridge, MA 02139
2	Southwest Research Institute ATTN: Mr. T. R. Jeter Dr. R. White Energetics Systems P.O. Box 28510 San Antonio, TX 78284
1	Batelle Northwest ATTN: Mr. M. Garnich P.O. Box 999 Richland, WA 99358
1	Lockheed Company ATTN: Mr. John Gerky P.O. Box 33, Dept. 1/330 Ontario, CA 91761
1	AAI Corporation ATTN: Dr. T. Stastney P.O. Box 6767 Baltimore, MD 21204
2	United States Military Academy Department of Mechanics ATTN: LTC Andrew L. Dull LTC Thomas Kiehne West Point, NY 10996

Aberdeen Proving Ground

Dir, USAMSAA
ATTN: AMXSY-D
AMXSY-MP, H. Cohen

Cdr, USATECOM
ATTN: AMSTE-TO-F

Cdr, CRDEC, AMCCOM
ATTN: SMCCR-RSP-A
SMCCR-MU
SMCCR-SPS-IL

USER EVALUATION SHEET/CHANGE OF ADDRESS

This laboratory undertakes a continuing effort to improve the quality of the reports it publishes. Your comments/answers below will aid us in our efforts.

1. Does this report satisfy a need? (Comment on purpose, related project, or other area of interest for which the report will be used.) _____

2. How, specifically, is the report being used? (Information source, design data, procedure, source of ideas, etc.) _____

3. Has the information in this report led to any quantitative savings as far as man-hours or dollars saved, operating costs avoided, or efficiencies achieved, etc? If so, please elaborate. _____

4. General Comments. What do you think should be changed to improve future reports? (Indicate changes to organization, technical content, format, etc.) _____

BRL Report Number _____ Division Symbol _____

Check here if desire to be removed from distribution list. ____

Check here for address change. ____

Current address: Organization _____
Address _____

----------FOLD AND TAPE CLOSED----------

Director
U.S. Army Ballistic Research Laboratory
ATTN: SLCBR-DD-T(NEI)
Aberdeen Proving Ground, MD 21005-5066

OFFICIAL BUSINESS
PENALTY FOR PRIVATE USE $300

BUSINESS REPLY LABEL
FIRST CLASS PERMIT NO. 12062 WASHINGTON D.C.
POSTAGE WILL BE PAID BY DEPARTMENT OF THE ARMY

NO POSTAGE NECESSARY IF MAILED IN THE UNITED STATES

Director
U.S. Army Ballistic Research Laboratory
ATTN: SLCBR-DD-T(NEI)
Aberdeen Proving Ground, MD 21005-9989